

The Unusual, Lepidosome-coated Resting Cyst of *Meseres corlissi* (Ciliophora: Oligotrichea): Genesis of Four Complex Types of Wall Precursors and Assemblage of the Cyst Wall

Wilhelm FOISSNER and Maria PICHLER

Universität Salzburg, FB Organismische Biologie, Salzburg, Austria

Summary. We studied the genesis of the cyst wall precursors and the assemblage of the cyst wall in *Meseres corlissi* Petz and Foissner (1992), an oligotrichous ciliate closely related to the common *Halteria grandinella*, using transmission electron microscopy. *Meseres corlissi* has five types of cyst wall precursors, of which type (A), the lepidosomes of the pericyst, has been described by Foissner *et al.* (2006). Each precursor type has a complex genesis showing six to nine distinct stages described in detail. Types (A) and (C) develop from Golgi vesicles, while the origin of types (B), (D) and (E) remains obscure. None of the precursors is similar to those reported from other ciliates, suggesting the oligotrichs as a very distinct group of ciliates. Except of precursor (E), they develop and release their contents almost concomitantly by exocytosis, whereby the precursor membrane closes the exocytotic openings and the contents lose the property to be stained with the usual dyes. Thus, the assemblage of the cyst wall, which suddenly “condenses” out off the mass formed by the extruded contents of the wall precursors, could be followed only during the last stages when the precursor materials became stainable again. There is cortex reorganization and intense perilemma endocytosis before the cyst wall assembles, events not described in any other study. Thus, the perilemma is a real structure whose function, however, remains obscure. Based on the present and literature data, a high morphological diversity of cyst wall precursors and wall assemblage emerges. If this variety is added to that of overall cyst morphology (e.g., wall ornamentation), cyst wall composition (e.g., with or without chitin) and cell restructuring (e.g., the infraciliature may be maintained or resorbed), an overwhelming diversity emerges which should contain considerable phylogenetic and ecological information; unfortunately, the message is only partially understood, likely because detailed data are available from less than 40 species.

Key words: cortex reorganization, diversity, exocytosis, oligotrichine ciliates, perilemma endocytosis, phylogeny, review.

INTRODUCTION

Resting cysts are a special mode of protists to overcome detrimental periods of life. Thus, their morphology, physiology, and ecology are of wide interest and have been reviewed under several aspects (Corliss

and Esser 1974, Foissner 1993, Chessa *et al.* 1994, Gutiérrez and Martín-González 2002, Gutiérrez *et al.* 2003).

Attempts to use the morphological diversity of resting cysts for classifying higher systematic categories of ciliates are still at variance (Foissner 2005), while their value in distinguishing morphologically very similar species is increasingly acknowledged (Foissner 1993, Foissner *et al.* 2002, Xu and Foissner 2005). Our unpublished data even suggest that applying this feature more commonly will double the number of free-living ciliate species! For

Address for correspondence: Wilhelm Foissner, Universität Salzburg, FB Organismische Biologie, Hellbrunnerstrasse 34, A-5020 Salzburg, Austria; E-mail: Wilhelm.Foissner@sbg.ac.at

instance, four very similar populations of *Epispathidium amphoriforme*, a common moss and soil ciliate, have different resting cysts, suggesting classification as different species.

The morphological literature on resting cysts is comparatively rich for colpodid and stichotrichine ciliates (for reviews, see Foissner 1993, Berger 1999, Gutiérrez *et al.* 2003), while scant for oligotrichs, such as *Tintinnidium*, *Halteria* and *Meseres*. None the less, the few data available indicate a great diversity: the cysts may be globular (Foissner *et al.* 2005) or flask-shaped (Reid and John 1978, 1983; Jonsson 1994; Kim and Taniguchi 1995; Müller 1996, 2002); the cysts may have (Fauré-Fremiet 1948; Reid and John 1978, 1983; Kim and Taniguchi 1995; Müller 1996, 2002; Montagnes *et al.* 2002) or lack (Foissner *et al.* 2005) an escape opening; the cysts may have (Foissner *et al.* 2005) or lack (Fauré-Fremiet 1948, Reid and John 1978, Jonsson 1994) lepidosomes, that is, the cyst wall is smooth or covered with globular or spiny scales; the cyst wall may have (Reid 1987) or lack (Foissner 2005) a crystalline, calcium-rich layer; the cyst wall may have (Foissner *et al.* 2005) or lack (Foissner, unpubl. data on *Halteria*) a chitinous layer; and the endocyst may strongly swell (Foissner *et al.* 2005) or not swell (Fauré-Fremiet 1948, Jonsson 1994) during excystment.

We used *Meseres corlissi*, a close relative of the common *Halteria grandinella* (Katz *et al.* 2005), as a model to investigate encystment and cysts of oligotrich ciliates (Foissner 2005; Foissner *et al.* 2005, 2006; Müller *et al.* 2006). These investigations showed that the resting cyst of *M. corlissi* is unusual in having a chitinous layer in the wall and a pericyst with conspicuous, up to 15 µm large scales, now called lepidosomes (Foissner 2005, Foissner *et al.* 2005). The lepidosomes have a complex genesis in Golgi vesicles and are released by exocytosis (Foissner *et al.* 2006). The present study shows two further peculiarities: there are five types of complex cyst wall precursors, while other ciliates have four or less types with comparatively simple morphology and genesis; and there is cortex reorganization and intense perilemma endocytosis before the cyst wall condenses, events not described in any other study.

All these investigations were extraordinarily difficult and time-consuming because oligotrichs are notoriously difficult to prepare for transmission electron microscopy and five types of cyst wall precursors, each with six to nine distinct developmental stages in at least two orientations (longitudinal and transverse), had to be sorted.

This required investigating 25 different fixatives; sectioning of nearly 100 vegetative, precystic and cystic specimens; and analyzing more than 3000 micrographs.

MATERIALS, METHODS AND TERMINOLOGY

Material and cultivation. The population studied was isolated from meadow soil of Upper Austria, i.e., from the surroundings of the town of Kefermarkt, using the non-flooded Petri dish method (Foissner *et al.* 2002).

A culture of *M. corlissi* was established with about 20 cells on Eau de Volvic (French table water) enriched with some squashed wheat grains and *Cryptomonas lucens* (UK Culture Collection of Algae and Protozoa, CCAP, Windermere) as food sources. Cultivation occurred at room temperature and day light. The first, asexual culture was used for all investigations because preservation of the fine structure distinctly decreases after even short periods of cultivation.

Induction of encystment. The various encystment stages were obtained by transferring about 2000 specimens from the exponentially growing culture with about 10% dividers into a Petri dish 5 cm across, together with 7 ml culture medium and the food contained therein. This isolated part of the culture was then controlled hourly with a dissecting microscope. Encysted specimens were recognized already after 5 hours, but epidemic encystment occurred after 20 hours when food was visibly reduced.

Morphological and cytological methods. For electron microscopy, the encysting culture mentioned above was fixed and embedded in toto as described in Foissner (2005). Briefly, cells were fixed in a mixture of 10 ml glutaraldehyde (25 %) + 6 ml aqueous osmium tetroxide (2 %) + 10 ml saturated aqueous mercuric chloride for 1 h and embedded in Epon 812 via a graded ethanol series and propylene oxide.

Six distinct stages can be distinguished during encystment (Foissner *et al.* 2006). Unfortunately, trials to trigger and synchronize the process failed. Thus, the appropriate stages were selected from the encysting, fixed and embedded culture described above, using a bright field microscope and a magnification of up to 250×.

Morphometry. As in our previous studies (Foissner 2005, Foissner *et al.* 2006), we provide basic morphometrics and statistics for the structures described. This is uncommon in cyst research and was criticized by some reviewers. However, we defend such data because they are much better, in spite of all the shortcomings they have, than the vague "about" so frequently seen in cyst literature. Furthermore, in the present study such data were indispensable for distinguishing the many developmental stages of the five cyst wall precursor types. For a more detailed discussion, see Foissner *et al.* (2006).

Terminology. General ciliate terminology follows Corliss (1979); cytological terminology is according to Plattner and Hentschel (2002) and Becker *et al.* (2006); and cyst terminology follows Gutiérrez *et al.* (2003), Foissner (2005), and Foissner *et al.* (2005). The various cyst wall precursors are termed « A, B, C, D, E » because we could not assign them to certain cyst layers, except of the (A) precursor which is the lepidosome and whose genesis has been described by Foissner *et al.* (2006).

RESULTS

Organization of description and morphometry (Fig. 1)

The vegetative species and its mature resting cyst have been described by Petz and Foissner (1992), Foissner (2005), and Foissner *et al.* (2005). The genesis and release of cyst wall precursor (A), that is, the lepidosomes, has been studied by Foissner *et al.* (2006).

Although precursor genesis is a continuous process, we distinguished several stages within each precursor type to emphasize the changes occurring and to make the description more clear. Further, the stages roughly correlate with the six encystment stages (Fig. 1) and may help to define the processes properly in more detailed research. Classifying a continuous process into

several stages is not uncommon. For instance, larval development is classified in over 40 stages in tadpoles.

The variability coefficients of mature structures of ciliates, for instance, body size and the number of ciliary rows, are usually between 5-15 % (Foissner 1984, 1993). In the present study, many variability coefficients are between 15 % and 30 %. Likely, this has several reasons: (i) the “stages” measured belong to a continuous process; (ii) some distinct stages may have been lumped; (iii) the maximum dimension of the structures may have been missed, though we measured only such precursors where crisp membrane profiles were recognizable, indicating that we were in or near to the centre.

The data compiled in Tables 1 and 2 and in Foissner *et al.* (2006) show that the five precursor types can be distinguished by their size, except of types (B) and (D): (A) 5842 × 4904 nm, (B) 1881 × 1363 nm, (C) 1734 ×

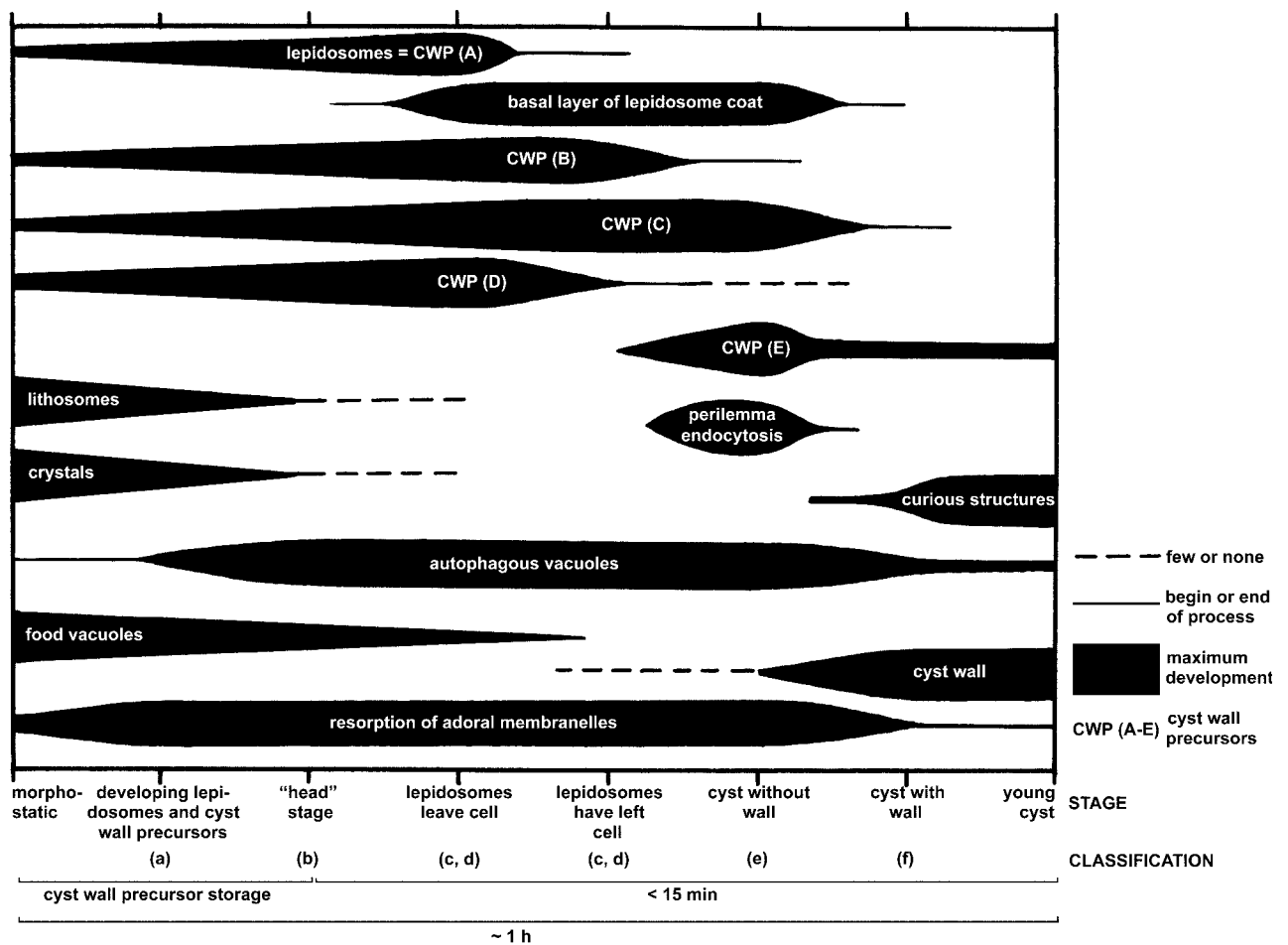


Fig. 1. *Meseres corlissi*, semiquantitative view of changes occurring during encystment. Note that the genesis of the lepidosomes has been described by Foissner *et al.* (2006); other structures not contained in the present study will be described in a forthcoming paper. Classification of encystment stages (a-f) is according to Foissner *et al.* (2006). See text for details.

257 nm, (D) 1855 × 1571 nm, (E) 443 × 293 nm. These data match those obtained from protargol-impregnated specimens, where all precursors can be seen (Figs 2, 3), except of precursor (E).

When encystment commences and the cyst wall precursors develop, the distinctness of the endoplasmic reticulum and the Golgi stacks strongly increases, as compared to morphostatic cells (Figs 32-34, 36, 39). The ordinary appearance is regained after the "head stage" (Foissner *et al.* 2006), that is, just before the lepidosomes are released.

Time course and relationship of processes (Fig. 1)

Encystment causes a complete transformation of the vegetative cell. Based on our previous investigations (Foissner 2005; Foissner *et al.* 2005, 2006), the present results, and some data from a forthcoming paper (Foissner and Pichler, in preparation), we are able to provide a scheme on the sequence and relationship of various main events occurring during encystment (Fig. 1). The time scale refers to the shortest period the processes can run. This was observed in specimens from the Dominican Republic, which were cultivated at 20-25°C (Weisse 2004). When transferred to 5°C, most specimens formed a mature resting cyst within 1 h (Foissner *et al.* 2005), while the cysts used for the present investigations were obtained after about 20 h from specimens kept at room temperature under decreasing food concentration (Foissner *et al.* 2006).

Protargol preparations show that cyst wall precursors are generated throughout the cell, but are most abundant in the broad anterior third (Figs 2, 3). As concerns the cyst wall precursors, types (A) to (D) are produced and released almost concomitantly, while precursor (E) is produced and released distinctly later (Fig. 1). Timing of precursors (A) to (D) is hampered not only by their almost concomitant production but also by cyst wall precursor storage, a remarkable phenomenon which will be described in a separate paper. Briefly, about one third of the specimens from exponentially growing cultures contain various developmental stages of precursor types (A) to (D); 10 % even contain few to many fully or almost fully differentiated precursors (Figs 2, 3).

Cyst wall precursor (B)

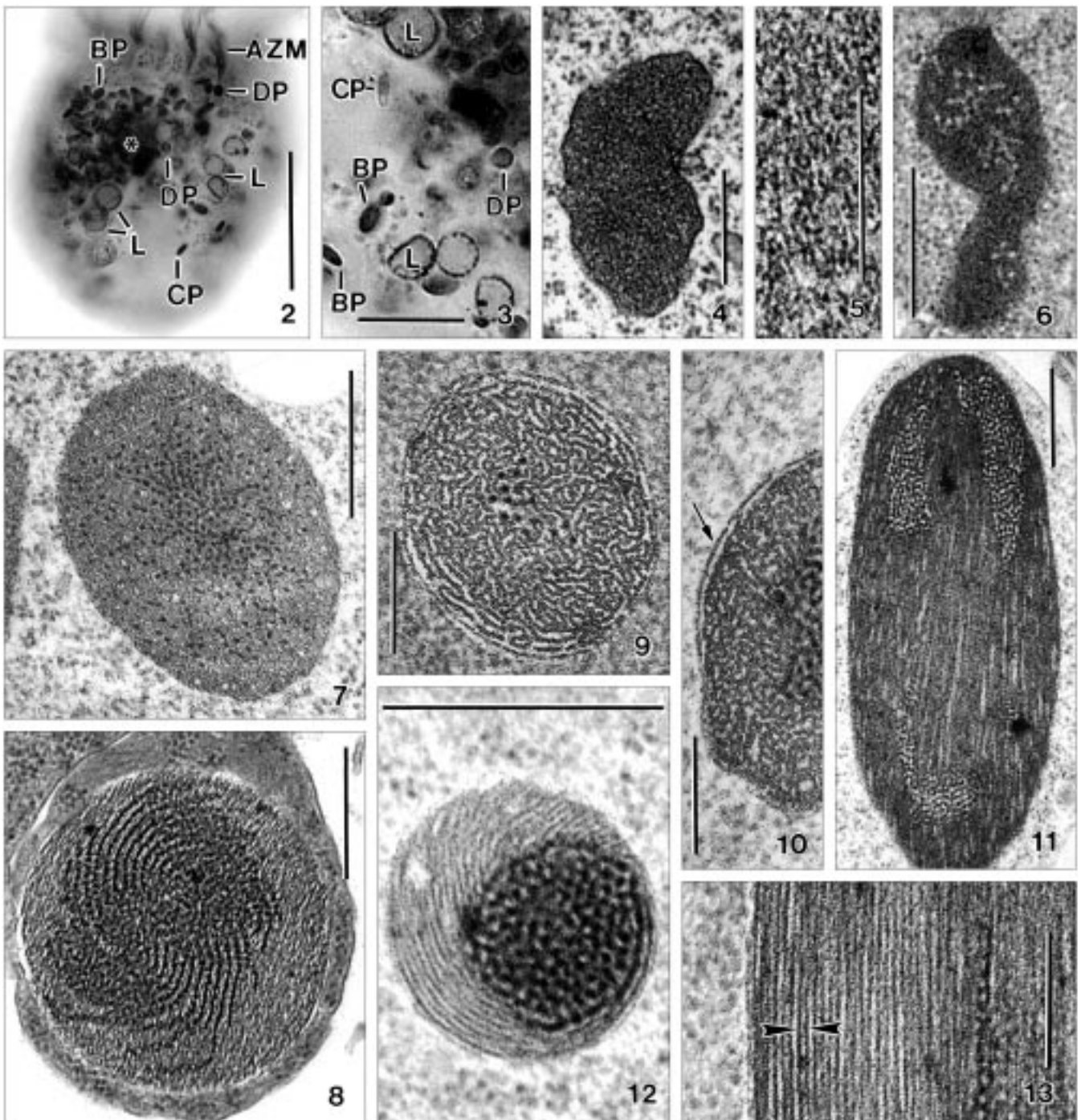
The cyst wall precursor (B) is generated together with precursors (A), (C) and (D), and released slightly later or almost concomitantly with precursor (A), that is, the lepidosomes. Precursor (B) is the largest precursor type, except of the lepidosomes, and is well recognizable

with the light microscope in protargol-impregnated specimens (Figs 2, 3). Beginning with stage (3), cyst wall precursor (B) is composed of a membranous matrix and fibrogranular material forming various patterns during the precursor's development. The about 12 nm thick sheets of the matrix are three-layered, that is, are composed of two osmiophilic outer layers and a bright inner layer each about 4 nm thick (Fig. 13). This composition is likely because three-layered sheets are distinct also in stage 8 (Figs 30, 31) and in some stages of the (C) precursor (Figs 35, 38, 40-42, 54).

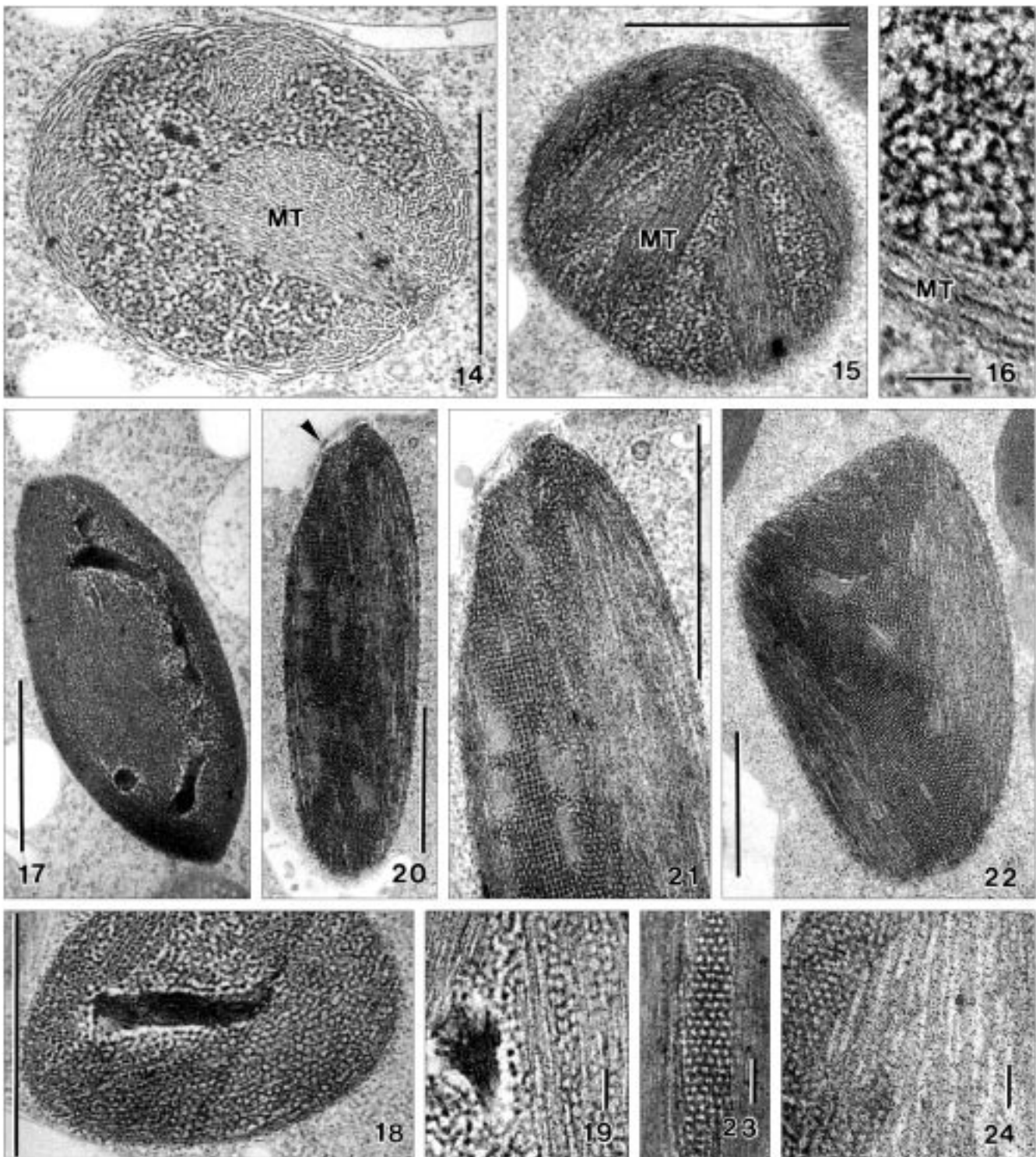
Stage (1): the earliest stages identified are roughly reniform, membrane-bound, dark vesicles with a rather irregular outline and an average size of 902 × 343 nm (Figs 4-6; Table 1). The vesicles are filled with amorphous or finely granular material; however, the best preparations reveal very narrowly meshed fibrous structures with a diameter of ≤ 2 nm (Figs 4, 5). In the central thirds of the vesicles are minute (~ 20 nm), bright areas in 60 out of 90 precursors investigated (Fig. 6). Possibly, these areas, which have a diffuse margin and provide the precursor with a white-spotted appearance, are formed by loosening of the matrix.

Stage (2): the precursors become broadly ellipsoidal because the width increases to an average of 669 nm (Table 1). The matrix is as in stage (1), that is, white-spotted, but now contains arrays of dark granules with a diameter of about 13 nm (Figs 7, 8). The granules, which are usually more densely spaced in the central portion of the precursor, frequently form lamellar patterns; rarely do they appear randomly distributed. It seems possible that the granular arrays are part of long, irregularly coiled sheets or strands with granules arranged like pearls on a string.

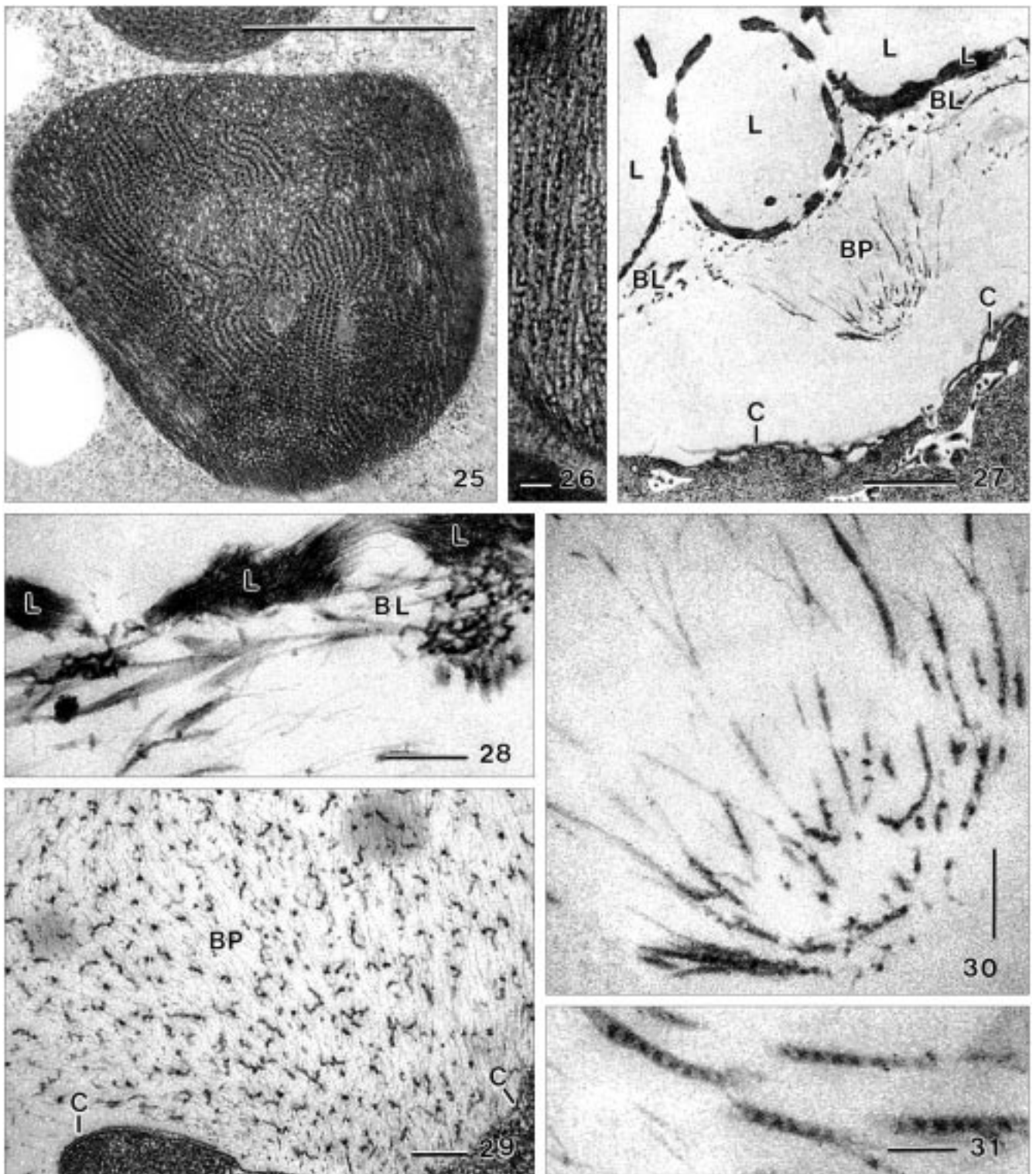
Stage (3): the precursors are now conspicuous, ellipsoidal to elongate ellipsoidal (2:1 - 6:1) structures of light microscopical dimension, that is, they have an average size of 2656 × 735 nm and rounded or bluntly pointed ends (Figs 9-12). Many transitions show that the great width variability (CV 45 %, Table 1) is natural, that is, not caused by lumping of two or more developmental stages. Longitudinal sections of well-preserved precursors now reveal the matrix as an array of bilamellate, membrane-like structures, as described above and shown in figure 13. Transverse sections show that the sheets are arranged in more or less pronounced sinuous patterns, making stage (3) highly distinct (Figs 9, 10); rarely, and mainly near to the ends of the precursor, the lamellae are helicoidally arranged (Fig. 12). The granular arrays described in stage (2) developed to a lobate, fibrogranular



Figs 2-13. *Meseres corlissi*, cyst wall precursors of morphostatic specimens in the light microscope (2, 3) and transmission electron micrographs of stages (1-3) of the genesis of cyst wall precursor (B) in encysting cells (4-13). **2, 3** - about 10 % of specimens from exponentially growing cultures contain developing lepidosomes (L) and cyst wall precursors (BP, CP, DP), which impregnate with protargol. The asterisk marks an accumulation of these structures; **4-6** - stage (1) cyst wall precursors (B) are reniform and have an average size of 902×343 nm. The osmiophilic, fibrogranular (4, 5) matrix often contains minute bright areas providing the precursor with a spotted appearance (6); **7, 8** - stage (2) precursors are broadly ellipsoidal and have an average size of 900×669 nm. Conspicuous granular arrays develop in the white-spotted matrix; **9-13** - stage (3) precursors are oblong (11) and have an average size of 2656×735 nm. The matrix now appears as an array of bilamellate, membrane-like structures (13, arrowheads) containing darkly stained, lobate areas of reticular, fibrogranular material (Figs 10-12). Transverse sections show that the lamellae form a sinuous or helical pattern (9, 10, 12). The arrow in figure 10 marks the membrane surrounding the precursor. AZM - adoral zone of membranelles, BP, CP, DP - cyst wall precursors, L -lepidosomes. Scale bars: 10 μ m (3); 30 μ m (2); 200 nm (5, 9, 10, 13); 400 nm (4, 6, 7, 8, 11, 12).



Figs 14-24. *Meseres corlissi*, transmission electron micrographs of stages (4-6) of the genesis of cyst wall precursor (B). **14-16** - stage (4) precursors are ellipsoidal and have an average size of 2450×1239 nm. In this stage, the lamellar matrix (MT) and the fibrogranular reticulum become strongly intertwined. Figure 14 shows a transition to stage (3), that is, the sinuous pattern of the matrix lamellae is still recognizable; **17-19** - stage (5) precursors are broadly ellipsoidal with an average size of 2343×1399 nm. Globular to oblong, compact inclusions appear in the fibrogranular reticulum and a honeycombed structure develops in the lamellar matrix; **20-24** - stage (6) precursors are ellipsoidal and have an average size of 2753×1080 nm. They are almost mature and thus typically found near or attached to the ciliate's cortex (20, arrowhead). Both, the fibrogranular reticulum and the compact inclusions recognizable in the previous stages have disappeared, while a highly characteristic, honeycombed structure developed throughout the precursor. MT - lamellar matrix. Scale bars: 1000 nm (14, 15, 17, 18, 20-22); 100 nm (16, 19, 23, 24).



Figs 25-31. *Meseres corlissi*, transmission electron micrographs of stages (7) and (8) of the genesis of cyst wall precursor (B). **25, 26** - mature (B) precursors have an average size of 1881×1363 nm, that is, are ellipsoidal to irregularly globular and composed of conspicuous granule strings sandwiched in two membranous sheets (Figs 26, 31); **27-31** - stage (8) comprises leaving and released precursors. As soon as the precursor is outside of the cell, it swells to a loose mass composed of countless fibres and wrinkled pieces (29) of the granule strings (30, 31). Likely, they form, after some transformation, the basal layer of the lepidosome coat (28). BL - basal layer, BP - cyst wall precursor (B), C - ciliate cortex, L - lepidosome and lepidosome wall. Scale bars: 100 nm (26, 30); 200 nm (28, 29, 31); 1000 nm (25, 27).

Table 1. Morphometric data on cyst wall precursors (B) and (C). Measurements in nm. CV - coefficient of variation in %, I - number of cysts investigated, M - median, Max - maximum, Min - minimum, n - number of precursors measured, SD- standard deviation, \bar{x} - arithmetic mean.

Characteristics	\bar{x}	M	SD	CV	Min	Max	n	I	
Precursor(B)									
Stage 1	length	902	900	173	19.2	600	1250	28	6
	width	343	300	96	28.0	250	600	28	6
Stage 2	length	900	850	183	20.3	700	1300	16	6
	width	669	600	178	26.6	400	1000	16	6
Stage 3	length	2656	2500	515	19.4	1800	3500	9	7
	width	735	600	332	45.1	300	1400	17	9
Stage 4	length	2450	2500	391	15.9	1800	3000	7	3
	width	1239	1200	184	14.9	950	1600	13	5
Stage 5	length	2343	2500	310	13.2	1700	2600	7	4
	width	1399	1300	306	21.9	1000	2100	14	8
Stage 6	length	2753	2900	650	23.6	1500	3800	15	3
	width	1080	1000	350	32.5	600	1750	15	3
Stage 7	length	1881	1787	531	28.2	1107	3000	10	4
	width	1363	1314	480	35.2	786	2000	10	4
Precursor(C)									
Stage 1	length	164	150	45	27.6	89	25	21	3
	width	85	75	27	32.0	49	147	21	3
Stage 2	length	399	384	104	26.2	267	600	10	2
	width	60	60	13	21.1	40	83	10	2
Stage 3	length	236	236	56	23.7	175	325	8	4
	width	177	170	37	20.9	133	232	8	4
Stage 4	length	274	282	50	18.3	211	320	4	2
	width	251	253	48	19.3	189	307	4	2
Stage 5	length	744	737	144	19.4	445	1000	18	4
	width	655	657	129	19.7	400	911	18	4
	length of dense strand	404	280	368	91.2	53	1429	28	4
	width of dense strand	149	138	58	38.9	55	267	26	4
	width of bright area	66	67	27	40.4	9	150	26	4
Stage 6	length	1576	1575	439	27.8	1000	2222	8	4
	width	404	415	112	27.8	240	573	8	4
Stage 7	length	1734	1689	202	11.7	1556	2000	4	3
	width	257	259	65	25.4	171	400	16	3
	length of dense plug	185	198	85	45.7	83	314	8	3
	width of dense plug	87	77	28	31.5	67	143	8	3
Stage 8	length	2338	2321	522	22.3	1450	3684	19	3
	width	275	267	61	22.1	200	421	19	3

reticulum extending in the anterior and posterior third of the precursor; rarely, the mass forms a rod-shaped array extending whole precursor length (Figs 10-12).

Stage (4): the precursors are now thicker than in stage (3) and have an average size of 2450×1239 nm (Table 1); likely, some are slightly flattened. In this stage, the lamellar matrix and the fibrogranular reticulum become intertwined, producing highly characteristic, irregular patterns; however, the lamellae still show a tendency to arrange longitudinally and peripherally (Figs 14, 15). Figure 14 shows a transition between stages (3) and (4), that is, the matrix lamellae are still sinuously arranged while the fibrogranular reticulum

forms a polygonal network with lobes distributed throughout the precursor (Figs 14-16).

Stage (5): the precursors are now broadly ellipsoidal and have a similar size as in stages (3) and (4), viz., 2343×1399 nm on average (Table 1). The overall fine structure is also as in stage (4), that is, the lamellar matrix and the fibrogranular reticulum are strongly intertwined, forming manifold patterns (Figs 17-19); the fibrogranular reticulum appears even more lobate than in stage (4), now extending between the individual lamellae of the matrix (Fig. 19). Stage (5) is characterized by the appearance of 1-7 (\bar{x} 2.8, $n = 27$) scattered, globular to oblong, dark inclusion in the fibrogranular reticulum

(Figs 17-19). These inclusions, which sometimes form long, lobate structures (Fig. 17), have an average size of 250×160 nm (n27) and possibly develop by uptake of electron-dense material in the meshes of the fibrogranular reticulum (Figs 17-19).

Stage (6): this stage appears when the lepidosomes are released or just left the ciliate (Foissner *et al.* 2006). The precursors now have an average size of 2753×1080 nm, and more than 90 % of them are near to or attached to the ciliate's cortex (Fig. 20, Table 1). The shape is highly variable: simple, short rods (Fig. 20) are side by side with oblong, polygonal precursors likely ready to be released (Fig. 22). The fine structure changed dramatically, that is, the fibrogranular reticulum (Figs 14-16) and the compact inclusions (Figs 17-19) recognizable in the previous stages have disappeared, while a highly characteristic, honeycombed structure with a mesh size of about 25 nm developed throughout the precursor and probably within the lamellar matrix (Figs 20-24). The (B)precursor now highly resembles "paracrystalline" ciliate mucocysts (Hausmann 1978).

Stage (7): usually, stage (7) is found in cells just having released the lepidosomes (Fig. 1). When the (B) precursor leaves the cell, it becomes globular to polygonal obtaining an average size of 1881×1363 nm (Table 1). Thus, the precursor is now shorter but thicker than in stages (5) and (6). The fine structure also changes considerably (Figs 25, 26). The honeycombed pattern arranges to highly characteristic strings composed of equidistantly spaced, about 12 nm-sized granules sandwiched between two membranous sheets each about 3 nm thick (Figs 25, 26); likely, the sheets represent the osmiophilic part of the matrix lamellae described in stage (3). This arrangement is well recognizable also in dissolving precursors (Fig. 30). The granule strings are embedded in fibrogranular, white-spotted material highly similar to that found in stage (2).

Stage (8): this stage comprises leaving and released precursors, which were found in four specimens having released the lepidosomes, suggesting that the (B) precursors are released slightly later than the (A) precursors (=lepidosomes). When leaving the cell, the vesicle's contents become loose and hyaline. As soon as it is outside, it swells to a globular mass up to 5 μ m across (Figs 27, 29). This mass, which accumulates at the proximal portion of the lepidosome coat, is composed of countless filaments and wrinkled pieces of the granular strings described in stage (7). Likely, the filaments are parts of the membranous sheets sandwiching the granule strings (Figs 30, 31). Soon, the filamentous

reticulum and the granule strings lose their staining property. Thus, their fate could not be followed, but likely they form the basal layer of the lepidosome coat (Figs 27, 28). The membrane surrounding the precursor vesicle becomes part of the ciliate cortex, as does that of the other precursors (Figs 59, 78; Foissner *et al.* 2006).

Cyst wall precursor (C)

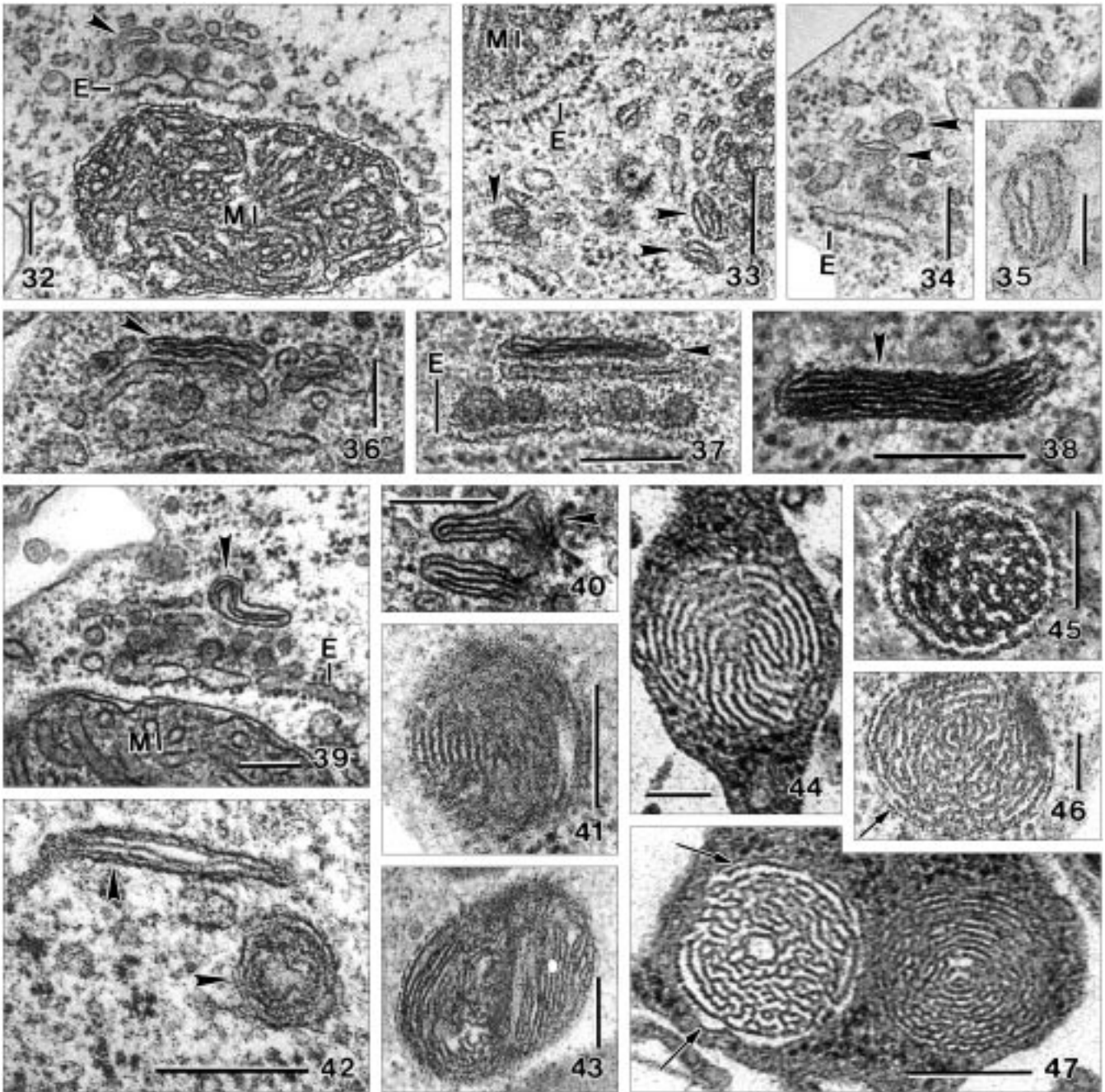
Cyst wall precursor (C) originates in vesicles of the Golgi apparatus, as does precursor (A). Its genesis is more complex and distinctive than that of the other precursors. Thus, the entire development process could be followed. In contrast, the structure is rather simple, i.e., the mature (C) precursor consists only of membranous sheets. Cyst wall precursor (C) is released slightly later than precursors (A), (B) and (D).

Stage (1): the first stage identifiable as developing (C) precursor is a broadly ellipsoidal vesicle at the distal side of the dictyosome (Fig. 32). These vesicles, which have an average size of 164×85 nm (Table 1), are made of a concentric array of two to three membranous lamellae, each about 6 nm thick and composed of two electron-dense sheets bordering an electron-lucent middle layer (Figs 32-35). Obviously, these vesicles were just produced by the dictyosome and migrated to the trans-Golgi network. No specific contents are recognizable between the lamellae (Fig. 35).

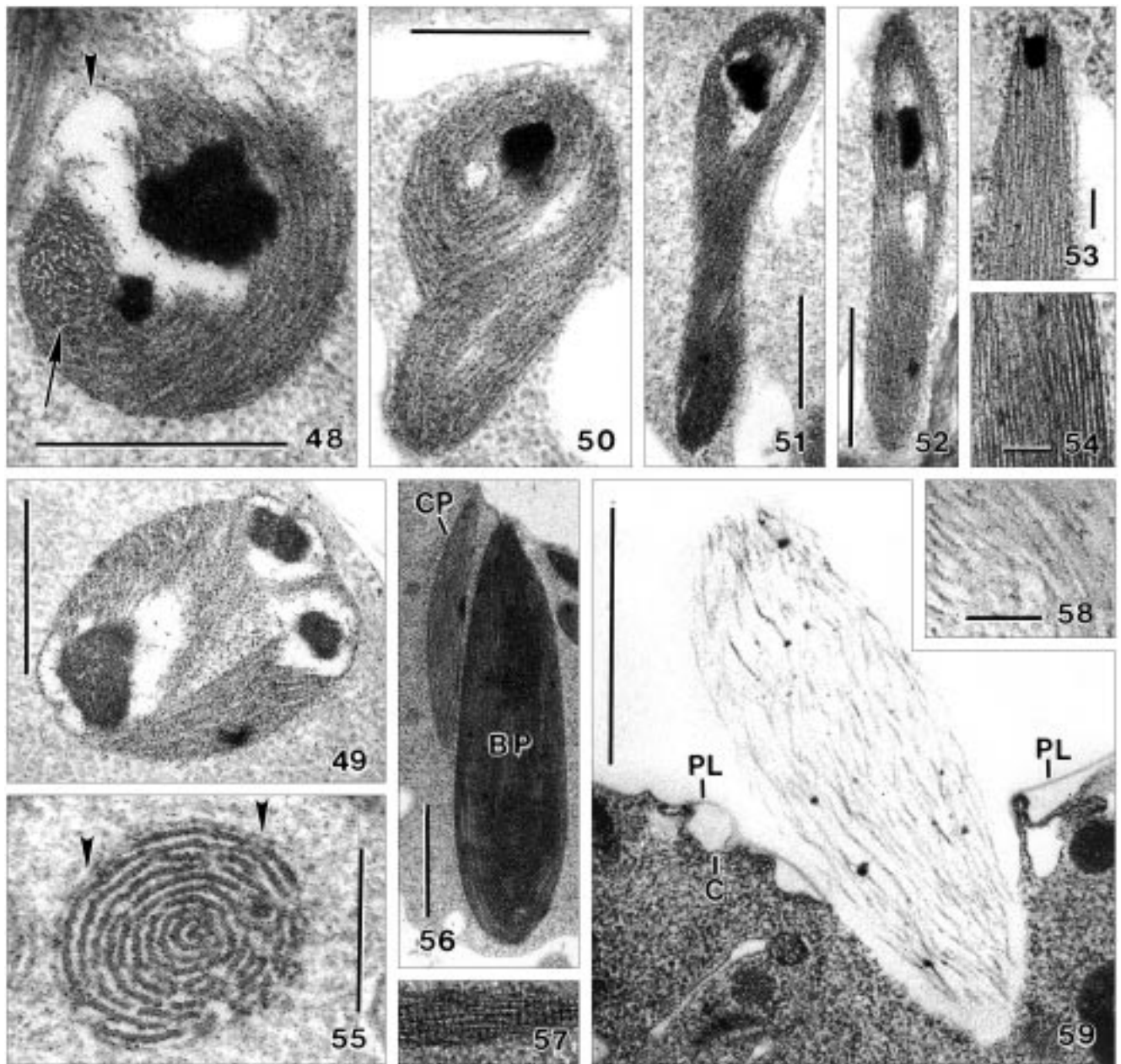
Stage (2): in stage (2), the globular vesicles of stage (1) grow to rod-shaped precursors with an average size of 399×60 nm (Figs 36-38, 42; Table 1). Like the stage (1) vesicles, they are at the distal side of the dictyosome and are composed of two to three concentric membranous lamellae. The space between the lamellae is clear.

Stage (3): the rod-shaped precursors of stage (2) roll up to broadly ellipsoidal, lamellar vesicles with an average size of 236×177 nm (Figs 39-43, Table 1). Likely, the involution occurs helically, as suggested by Fig. 43 and stage (6), where the vesicles unroll (Figs 48, 50). When reaching stage (4), the number of lamellae doubles and triples (Figs 41, 43).

Stage (4): the cyst wall precursors have grown to a size of 274×251 nm on average and became globular (Table 1). The membranous lamellae increased in number and form a conspicuous, sinuous pattern (Figs 44-47), highly similar to that found in stage (3) of the (B) precursor (Fig. 9). However, the stage (3) vesicles of the (B) precursor are much larger (2656×735 nm, Table 1) and usually contain a fibrogranular reticulum in the centre (Figs 9, 10, 12); further, we observed transi-



Figs 32-47. *Meseres corlissi*, transmission electron micrographs of stages (1-4) of the genesis of cyst wall precursor (C). **32-35** - the (C) precursor originates from vesicles of the trans-Golgi network on the distal side of the dictyosome (arrowheads). These vesicles have an average size of 164×85 nm and are composed of a concentric array of two to three membranous lamellae (Fig. 35). The active Golgi apparatus of *Meseres* is comparatively distinct and shows the classical structure, i.e., transition vesicles from the smooth surface of the endoplasmic reticulum form a Golgi stack composed of one to three cisterns. Note a coated transport vesicle (Fig. 33, asterisk); **36-38** - in stage (2), the ellipsoidal vesicles of stage (1) grow to rod-shaped precursors with an average size of 399×60 nm (arrowheads); **39-43** - during stage (3), the rod-shaped precursors of stage (2) roll up to broadly ellipsoidal, lamellar vesicles with an average size of 236×177 nm (Figs 39, 40, 42, arrowheads). Likely, the involution occurs helically (Fig. 43). Figure 42 shows a rod-shaped stage (2) precursor and a globular stage (3) precursor side by side (arrowheads). When reaching stage (4), the membranous lamellae double and treble (Figs 41, 43); **44-47** - stage (4) precursors have grown to an average size of 274×251 nm, that is, are globular. The membranous lamellae increased in number and form a sinuous pattern; note that the right precursor shown in figure (47) belongs to stage (8). Arrows mark the membrane surrounding the precursor. E - endoplasmic reticulum, MI - mitochondria. Scale bars: 100 nm (35); 200 nm (32-34, 36-46).



Figs 48-59. *Meseres corlissi*, transmission electron micrographs of stages (5-9) of the genesis and release of cyst wall precursor (C). **48, 49** - stage (5) cyst wall precursors (C) are globular and have an average size of 744×655 nm. The sinuous stage (4) matrix lamellae, remnants of which are recognizable in figure 48 (arrow), become helical and an electron-dense strand develops and appears in one to four pieces. Serial sections reveal the pieces as part of a peripheral helix performing one to two turns. Explanation of arrowhead in (48), see next figure; **50, 51** - stage (6) is characterized by the unfolding of the precursor. Unfolding commences with a blister (Fig. 48, arrowhead) and proceeds, via a retort-shaped transition stage (Fig. 50), to a rod-shaped vesicle with an average size of 1576×404 nm (Figs 51, 52, 56). The dense, peripheral helix present in stage (5) shortened to a small plug in the inflated anterior third of the precursor; **52, 53** - when approaching stage (7), the precursor has an average size of 1734×257 nm and is composed of a dense apical to subapical plug and 15-20 concentric, slightly helical lamellae; **54-56** - stage (8) precursors are mature and fusiform. They have an average size of 2338×275 nm and are thus three times thinner than the (B) precursors (Fig. 56). As concerns the fine structure, the fully developed (C) precursor is entirely composed of well preserved, concentric membranous sheets (lamellae) forming conspicuous arrays in transverse section (Figs 47, right specimen; 55, arrowheads mark the membrane surrounding the precursor); **57** - decomposing kinetodesmal fibres can be mixed up with late (C) precursors because they have a similar size and shape; **58, 59** (for an overview, see Fig. 107) - when released, the membranous sheets composing the (C) precursor lose their contour and dissolve. Unfortunately, the dissolved material does not stain, and thus we could not localize the cyst wall layer produced by the (C) precursor. BP - (B) cyst wall precursor, C - ciliate cortex, CP - (C) cyst wall precursor, PL - perilemma of the ciliate cortex. Scale bars: 100 nm (53, 54, 58); 200 nm (55); 500 nm (48-52); 1000 nm (56, 59).

tions between stages (4) and (5), excluding the possibility that the stage (4) precursors are misidentified (B) precursors (Fig. 48).

Stage (5): the (C) cyst wall precursor now reaches light microscopical dimension, that is, has an average size of 744×655 nm (Table 1); likely, most are globular. The fine structure changes markedly, that is, the sinuous matrix lamellae become helical and an electron-dense strand develops (Figs 48, 49). Usually, the matrix lamellae are poorly preserved, as compared to former and later stages, indicating that the transition from the sinuous to the helical state is still in progress. The dense strand appears in form of one to four scattered pieces or as a conspicuous semicircle (Figs 48, 49). Serial sections reveal the pieces as part of a peripheral helix performing one to two turns. The strand, which consists of a very fine-grained, heavily osmiophilic substance, has an irregular outline and an average width of 150 nm. It is surrounded by an about 66 nm wide bright zone traversed by many fibrogranular filaments connecting strand and matrix (Figs 48, 49; Table 1). When the precursor commences unfolding (see next stage), an electron-lucent blister becomes recognizable (Fig. 48, arrowhead).

Stage (6): now a remarkable process commences, viz., the globular vesicle unfolds, showing the helical arrangement of the matrix lamellae proposed in stage (3). Unfolding commences with an electron-lucent blister (Fig. 48, arrowhead) and proceeds via a retort-shaped transition stage (Fig. 50) to a clavate vesicle with an average size of 1576×404 nm (Fig. 51, Table 1). The clavate precursor is helically wound about the main axis and has a dense, globular plug embedded in the inflated anterior portion. Usually, the matrix lamellae are poorly preserved, suggesting that their reconstruction is still in progress. Further, the lamellae are usually absent from the centre and from small, scattered areas throughout the precursor, likely representing the sites of the dense peripheral helix (see previous stage), which shortened to the plug described above.

Stage (7): the (C) precursor is almost mature and has a size of 1734×257 nm on average, that is, it is rod-shaped and frequently attached to the cortex of the ciliate at angles ranging from perpendicular to almost parallel to the cell's surface. The precursor is now composed of a dense apical to subapical plug with an average size of 185×87 nm (Table 1) and 15-20 concentric, slightly helically arranged matrix lamellae (Figs 52, 53).

Stage (8): the mature stage (8) precursors are fusiform and can be recognized in the light microscope because they have an average size of 2338×275 nm (Figs 2, 3). As compared to the (B) precursors, the (C) precursors have a similar length but are three times thinner (Fig. 56, Table 1). The dense plug and the surrounding bright area disappear (Fig. 56), the membranous lamellae arrange longitudinally (Figs 54, 56), and the interlamellar space becomes clear (Figs 54, 56), showing that the reconstruction of the lamellae has finished. Thus, the fully differentiated (C) precursor is entirely composed of well preserved, about 6 nm thick, concentric membranous sheets (lamellae) forming conspicuous arrays in transverse section (Figs 47, right specimen; 55). They are easily mixed up with decaying kinetodesmal fibres which, however, usually have a distinct transverse striation (Fig. 57).

Stage (9): the (C) precursor is released slightly later than the lepidosomes, leaving its contents in a 1-3 μ m thick zone between the globular, encysting cell and the lepidosome coat. The membrane sac surrounding the precursor becomes part of the cortex, while the contents swell to an oblong mass with a size of about 2300×800 nm, that is, the length remains similar to that of the attached state, while width doubles; attachment and release of the precursor occur in a wide variety of angles, as described in stage (7). The emerging contents soon become a spongy mass with fading contours (Figs 58, 59). When the mass touches the lepidosome coat, it dissolves and seemingly disappears, that is, loses the property to be stained with uranyl acetate, lead citrate, and bismuth, quite similar to the other precursors (Fig. 27). When precursor release is disturbed by the fixation shock, the emerging contents often become enclosed in a sheet of cortical perilemma; rarely, the precursor explodes within the cell, showing that the membranous lamellae become "unsharp", that is, lose their integrity because they commence to dissolve.

Cyst wall precursor (D)

The very early and early developmental stages of the (D) precursor were difficult to identify. Thus, we performed a retrospective analysis using stage (4) as a template. This and the specific vesicle membrane [see stage (1)] clarified the early stages, while the very early stages remained obscure.

Stage (6) of the (D) precursor is similar to stages (e) and (f) of the (A) precursor (=lepidosomes; Foissner *et al.* 2006): both have a thick, deeply stained peripheral

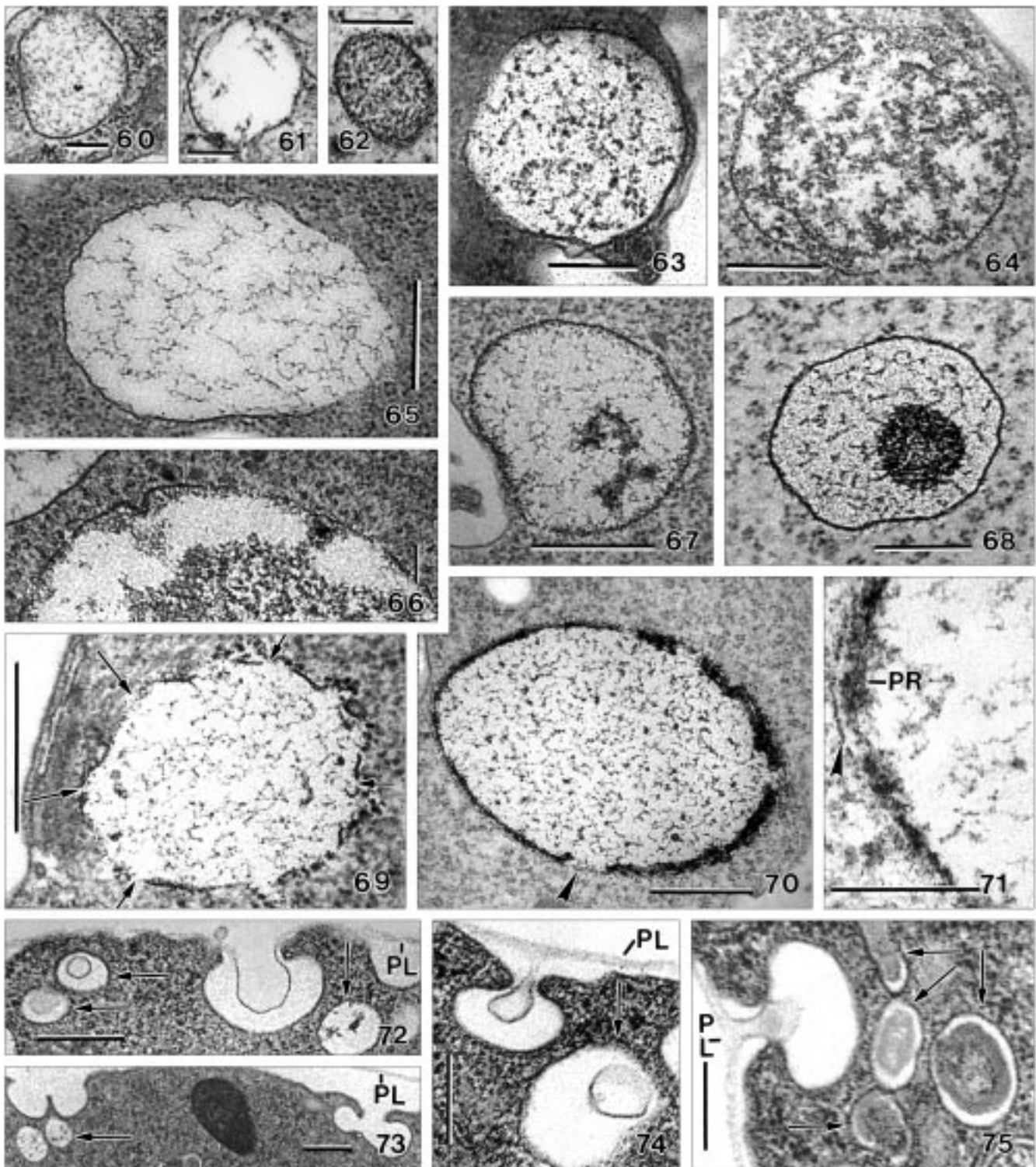
Table 2. Morphometric data on cyst wall precursors (D) and (E) of *Meseres corlissi*. Measurements in nm. CV - coefficient of variation in %, I - number of cysts investigated, M - median, Max - maximum, Min - minimum, n - number of precursors measured, SD- standard deviation, \bar{x} - arithmetic mean.

Characteristics	\bar{x}	M	SD	CV	Min	Max	n	I	
Precursor (D)									
Stage 1	length	323	296	153	47.3	147	524	8	6
	width	287	238	128	44.7	147	455	8	6
Stage 2	length	616	625	109	17.7	383	825	25	8
	width	505	548	113	22.4	308	700	25	8
Stage 3	length	1230	1161	389	31.7	683	2105	20	9
	width	960	889	306	31.9	483	1579	20	9
Stage 1-3	vesicle membrane, thickness	8	7	2	31.4	4	15	59	14
Stage 4	length	1022	1089	254	24.9	600	1325	15	5
	width	757	778	177	23.4	500	1000	15	5
Stage 6	length	1647	1705	266	16.2	1107	2036	20	5
	width	1426	1409	204	14.3	1107	1786	20	5
Stage 7	length	1503	1429	331	22.0	933	2321	21	5
	width	1299	1250	296	22.8	750	2000	21	5
Stage 8	length	1855	1875	224	12.1	1367	2286	23	7
	width	1571	1556	278	17.7	867	2071	23	7
	small net, length	125	120	45	36.0	75	275	16	6
	small net, width	85	85	16	19.0	50	111	16	6
	granules in net, ϕ	13	13	2	15.4	8	18	16	6
Stage 9	length within cell	1248	1179	203	16.2	1100	1533	4	2
	width within cell	813	748	196	24.1	667	1089	4	2
Stage 9	length outside cell	1989	1737	521	26.2	1400	2750	9	1
	width outside cell	1552	1458	381	24.6	1105	2105	9	1
Precursor (E)									
Stage 1	length	261	267	75	28.6	160	464	14	3
	width	202	200	61	30.1	133	357	14	3
Stage 2	length	585	598	89	15.2	420	700	8	2
	width	382	409	61	15.9	293	444	8	2
Stage 3	length	533	500	116	21.7	417	778	12	4
	width	210	223	41	19.4	133	275	12	4
Stage 4	total length	532	536	94	17.5	314	679	22	2
	total width	351	356	70	20.1	143	464	22	2
	core length	269	267	71	26.4	114	428	22	2
	core width	238	247	51	21.4	100	321	22	2
Stage 5	total length	443	440	63	14.1	371	556	9	4
	total width	293	283	60	20.4	200	400	9	4
	core length	337	333	85	25.2	229	467	9	4
	core width	190	171	49	26.1	133	286	9	4

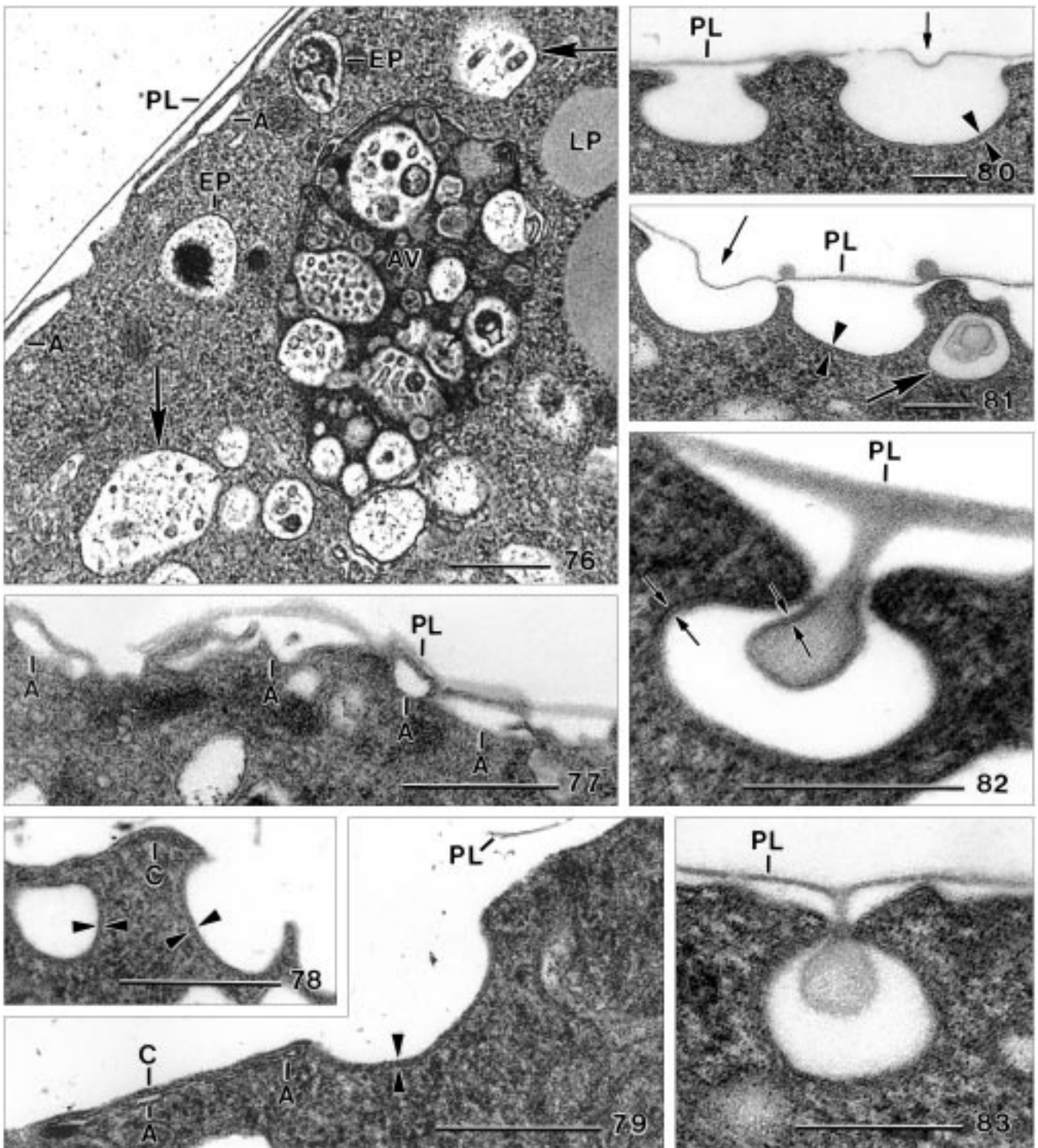
reticulum. However, they can be distinguished by three features. First, the lepidosomes have a thin, continuous base separating the wall meshes from the vesicle's contents. The (D) precursor lacks this base and thus the vesicle's contents are separated from the cytoplasm only by the membrane surrounding the vesicle (Figs 84, 85). Second, the peripheral reticulum of the (D) precursor develops on its surface (Figs 69-71, 84), while the reticulum of the lepidosome develops from the contents of the vesicle, that is, grows from the vesicle's centre to the periphery. Third, the fine structure of the peripheral

reticulum is different: very finely granular or filamentous in stage (e) and (f) lepidosomes, while distinctly reticular in the (D) precursor (Figs 84-86).

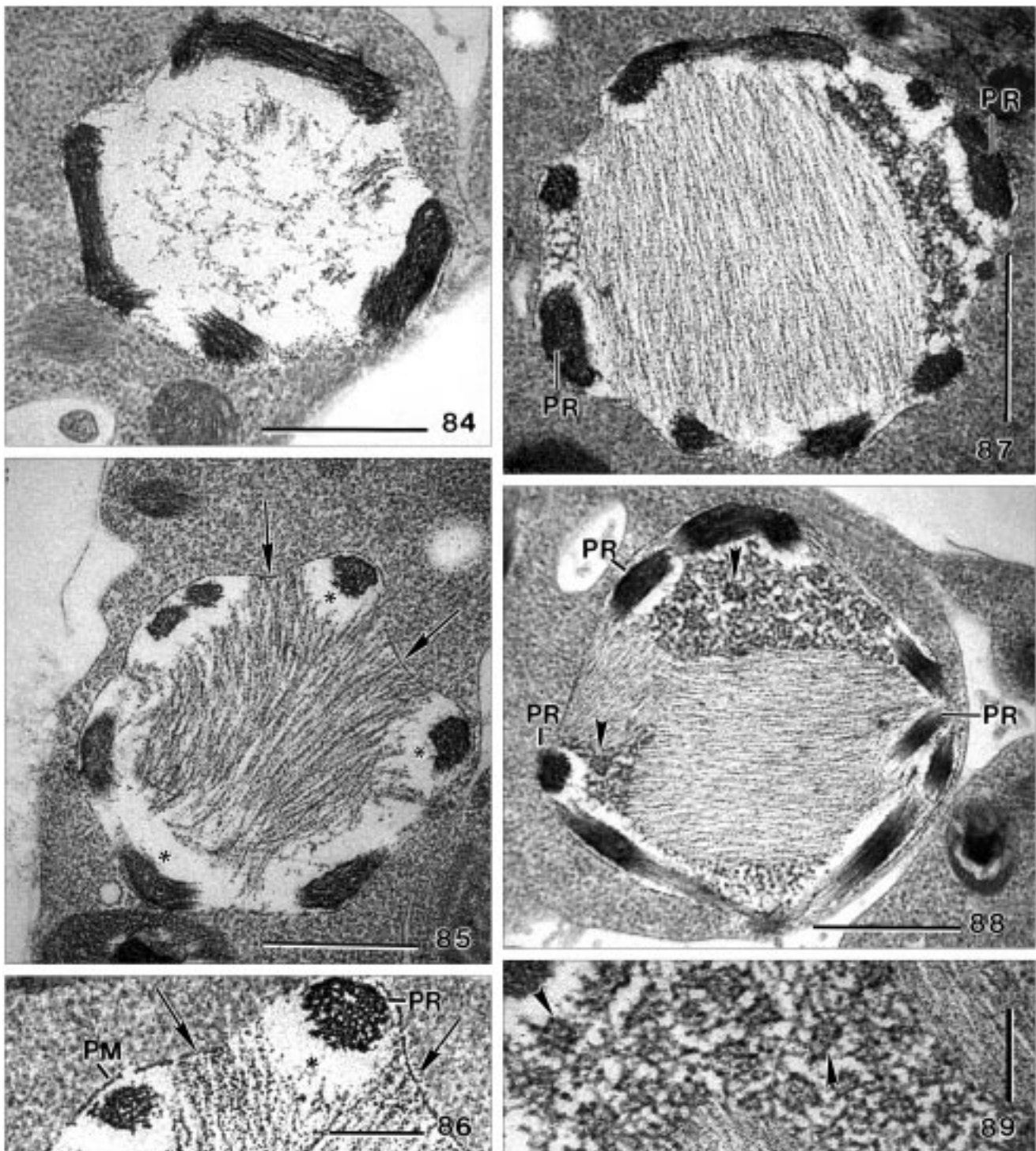
Stage (1): the earliest stage classified as developing (D) precursor are membrane-bound, slightly wrinkled vesicles with an average size of 323 × 287 nm (Table 2). The identification of the early development stages (1) to (3) is based not only on the retrospective analysis of stage (4), but mainly on the vesicle membrane which is more distinct (thicker) than in the corresponding stages of the other cyst wall precursors (Figs 60-68). Obviously,



Figs 60-75. *Meseres corlissi*, transmission electron micrographs of stages (1-5) of the genesis of the (D) cyst wall precursor (60-71) and of perilemma endocytosis (72-75). **60-68** - stage (1) to (3) vesicles differ mainly in size and have fibrogranular or alveolar contents. Note the characteristic, about 10 nm thick vesicle membrane; **69** - stage (4) precursors are unique in having bright areas in the vesicle membrane (arrows); **70, 71** - stage (5) shows that the osmiophilic membrane pieces recognizable in stage (4) become thicker, later forming the peripheral reticulum. Arrowheads mark the membrane surrounding the precursor. **72-75** - perilemma endocytosis during encystment stage (e; Fig. 1). Arrows mark internalized vesicles with decomposing perilemma. PL - perilemma, PR - growing peripheral reticulum. Scale bars: 200 nm (60-63, 66, 71, 74, 75); 400 nm (64, 65, 67-70, 72, 73).



Figs 76-83. *Meseres corlissi*, transmission electron micrographs of cortex reorganization (76, 77) and perilemma endocytosis (78-83). Opposed arrowheads mark the 12-22 nm thick coated membrane of endocytotic vesicles. Opposed arrows mark unit membranes of ordinary thickness (~ 6 nm). **76** - when cortical reorganization commences, the alveoli (A) become very distinct. Arrows mark large vesicles with decomposing perilemma. Note the large autophagous vacuole (AV); **77** - during reorganization, the cortex becomes heavily wrinkled and the alveoli increase in size; **78, 79** - forming endocytotic vesicles with coated wall (opposed arrowheads). The reorganized cortex has very small alveoli; **80-83** - perilemma endocytosis commences with a minute concavity (thin arrows) over the centre of the endocytotic vesicle (see also Figs 72-75). The thick arrow in (81) marks an internalized vesicle with perilemma. A - cortical alveoli, AV - autophagous vacuole, C - cortex, EP - (E) cyst wall precursor, LP - lipid droplet, PL - perilemma. Scale bars: 500 nm (76-79); 200 nm (80-83).



Figs 84-89. *Meseres corlissi*, transmission electron micrographs of stages (6) to (8) of the genesis of cyst wall precursor (D). **84** - stage (6) precursor vesicles have an average size of 1647×1426 nm and are thus recognizable in the light microscope (Figs 2, 3). The precursor now has a thick, dense peripheral reticulum encaging a loose, fibrogranular reticulum; **85, 86** - stage (7) is characterized by interwoven fibre bundles in the central two thirds of the precursor. The bundles are attached to the vesicle's membrane (arrows). The peripheral third of the precursor contains the loose, fibrogranular reticulum of stage (6), leaving an about 100 nm wide area (asterisks) around the branches of the dense peripheral reticulum (PR); **87-89** - stage (8) precursor vesicles have an average size of 1855×1571 nm. The central fibre bundles are straight and a fibrous network develops between the central bundles and the dense peripheral reticulum (Fig. 87). When fully developed, the network consists of roundish, narrowly meshed areas (arrowheads) within a more widely meshed basal network (Figs 88, 89). PM - precursor membrane, PR - dense peripheral reticulum. Scale bars: 200 nm (86, 89); 600 nm (84, 85, 87, 88).

some strongly osmiophilic material attaches to, or is contained in, the vesicle membrane which, indeed, is about 8 nm thick (Table 2), while ordinary organelle membranes are 6 nm thick (Sitte *et al.* 1991). This specialization is very likely related to the specific function the membrane has in the (D) precursor: it becomes the thick, strongly osmiophilic peripheral reticulum (see stages [4] and [5]). The vesicle's contents may be electron-lucent or fibrogranular forming an alveolar or smooth pattern (Figs 60-62). We found such vesicles in five specimens and with two fixation methods, suggesting that the varying aspect of the contents is not an artifact. However, the rather irregular outline of the vesicles may be caused by the coagulation of the cytoplasm.

Stage (2): this stage is very similar to stage 1, but the vesicles measure 616×505 nm on average, that is, doubled their size (Fig. 63, Table 2). When analyzed separately, the alveolar and finely granular vesicles have a very similar average size, suggesting that they represent a single vesicle type.

Stage (3): again, the size of the vesicles doubled, reaching light microscopical dimension, viz., 1230×959 nm on average (Table 2). Still, the vesicle's outline is rather irregular, while the contents are widely alveolar often showing denser, coarsely granular regions, sometimes even a dense globule (Figs 64-68).

Stage (4): the vesicles have similar size, shape, and contents as those of stage (3), but bright regions develop in the membrane (Fig. 69, Table 2). We could not clarify whether both, the membrane and the osmiophilic substance or only the latter disappear in these regions. Later stages show the bright areas as part of a coarse, peripheral reticulum (Figs 84, 85, 87, 88). This developmental stage is unique for the (D) precursor.

Stage (5): few stage (5) precursors were found, indicating rapid development between stages (3) to (6). The vesicles are similar to those of stage (4), but the wall is distinctly thicker (Figs 70, 71).

Stage (6): the (D) precursor has now an average size of 1647×1426 nm, that is, it is almost globular and recognizable in the light microscope (Figs 2, 3; Table 2). Morphologically, stage (6) is characterized by the thick, darkly stained peripheral reticulum, which is now fully developed (Fig. 84). The wall has an average thickness of 125 nm (SD 16.2, CV 13.0, Min 100, Max 150, $n = 15$) and is composed of fine fibres or sheets forming a reticular pattern in transverse section (Figs 84, 86). The vesicle's contents are lightly stained and show a loose,

fibrogranular reticulum, with a tendency to form more narrowly meshed, scattered accumulations.

Stage (7): there is further, slight growth of the precursor (Table 2). Stage (7) is characterized by the appearance of distinct fibre bundles mainly in the centre of the vesicle; many transitions occur between stages (6) and (7), suggesting comparatively slow development of the fibre bundles. When fully developed, the bundles are distinctly stained, more or less curved, and attached to the vesicle's membrane (Figs 85, 86). The fibres, which have a diameter of about 8 nm leave blank most of the peripheral third of the precursor, where the fibrogranular reticulum extends described in stage (6). This reticulum leaves blank an about 109 nm ($n = 16$) wide area around the peripheral reticulum, similar to the blank zone around the dense plug of the (C) precursor. However, both nets are connected by many fibrogranular strands (Figs 85, 86).

Stage (8): the (D) precursor is now fully developed and has an average size of 1855×1571 nm. Likely, most are globular because 40 % of the vesicles have a circular or nearly circular outline. Stage (8) is highly conspicuous and characterized by two features (Figs 87-89, Table 2): (i) the fibre bundles, which are now attached to both the vesicle's membrane and the peripheral reticulum, become straight and very dense, and (ii) the fibrogranular material between the fibre core and the vesicle's membrane becomes very distinct, forming a wide-meshed basal net containing many narrow-meshed areals with an average size of 125×85 nm. Many deeply stained granules with an average diameter of 13 nm are scattered in the net fibres. The peripheral reticulum is as described in stage (6).

Stage (9): the (D) precursors are released together with and slightly later than the lepidosomes. Just before extrusion, a series of changes occurs (Figs 90-92): the peripheral reticulum disappears without leaving any recognizable material; the fibres composing the central area reduce the diameter from about 8 nm in stage (8) to 4 nm in stage (9) and become reticular; the net around the central fibre core disappears, except of the narrowly meshed areas, which form highly characteristic curls, each composed of a wrinkled fibre and scattered, deeply stained granules; and the precursor decreases from an average size of 1855×1571 nm in stage (8) to 1247×813 nm in stage (9), likely due to the cell turgor which compresses the vesicle after the dissolution of the peripheral reticulum (Figs 90-92, Table 2). All these processes occur during a minute or so, that is, when the

lepidosomes are released, and they can be considerably altered by the fixation shock (see below).

As soon as the cortex opens, the cell turgor presses the contents of the precursor into the space between cortex and lepidosome coat, while the precursor membrane becomes part of the cortex. The perilemma opens like the other cortex membranes (Figs 90, 91); no specific structures are recognizable around the port. The further events could not be followed because the precursor's contents soon become stainless.

As mentioned above, the fixation shock can alter the processes considerably. Almost half of the 15 precursor extrusions seen still have the peripheral reticulum, both inside and outside the cell, where it disappears rapidly. That such stages are artifacts is indicated by the perilemma, which sometimes encages the extruded material.

Cyst wall precursor (E)

The (E) precursor appears late and is short-lived, that is, it becomes recognizable when the lepidosomes and the other cyst wall precursors have been released and disappears when the cyst wall develops, though late developmental stages are still recognizable in some young cysts (Fig. 1). They are numerous, i.e., there are about 80.000 (E) precursors in a cell, as calculated from their average size (~500 nm), the thickness of the sections (~80 nm), and the number of cuttings (~200) found in a transverse section through the middle third of a specimen. Further, (E) precursors are the simplest and smallest out of the five precursor types found. Thus, they reach the final size (~500 nm) already in developmental stage (2). During genesis of the (E) cyst wall precursor, cortex reorganization and perilemma endocytosis occur, as described below.

Stage (1): the first stage recognizable is a small, membrane-bound, rather distinctly wrinkled, bright vesicle with an average size of 261×202 nm (Figs 93, 94; Table 2). The origin of these vesicles could not be clarified. The fibrogranular contents form a wide-meshed pattern. Near the vesicle's margin, the contents show one or two minute, dark (electron-dense) accumulations, which distinguish this vesicle type from other ones.

Stage (2): the vesicles have grown to 585×382 nm on average, which is already the mature size (Table 2). They have a slightly wrinkled membrane and are pyriform (Figs 95, 96), a unique shape not found in any other precursor type of *Meseres*. As in stage (1), the fibrogranular contents form comparatively large alveoli

which, however, become filled with strongly osmiophilic material in the broader half of the precursor. Thus, this stage is conspicuously spotted (Figs 95, 96).

Stage (3): next, the precursor becomes ellipsoidal to oblong, i.e., gets an average size of 533×210 nm and a length:width ratio ranging from about 1.5:1-3.5:1 (Table 2). The vesicles have a rather wrinkled membrane and a bright, fibrogranular fringe. The central half is filled with darkly stained, narrowly meshed material, emphasizing the rod-like appearance of the precursor (Fig. 97).

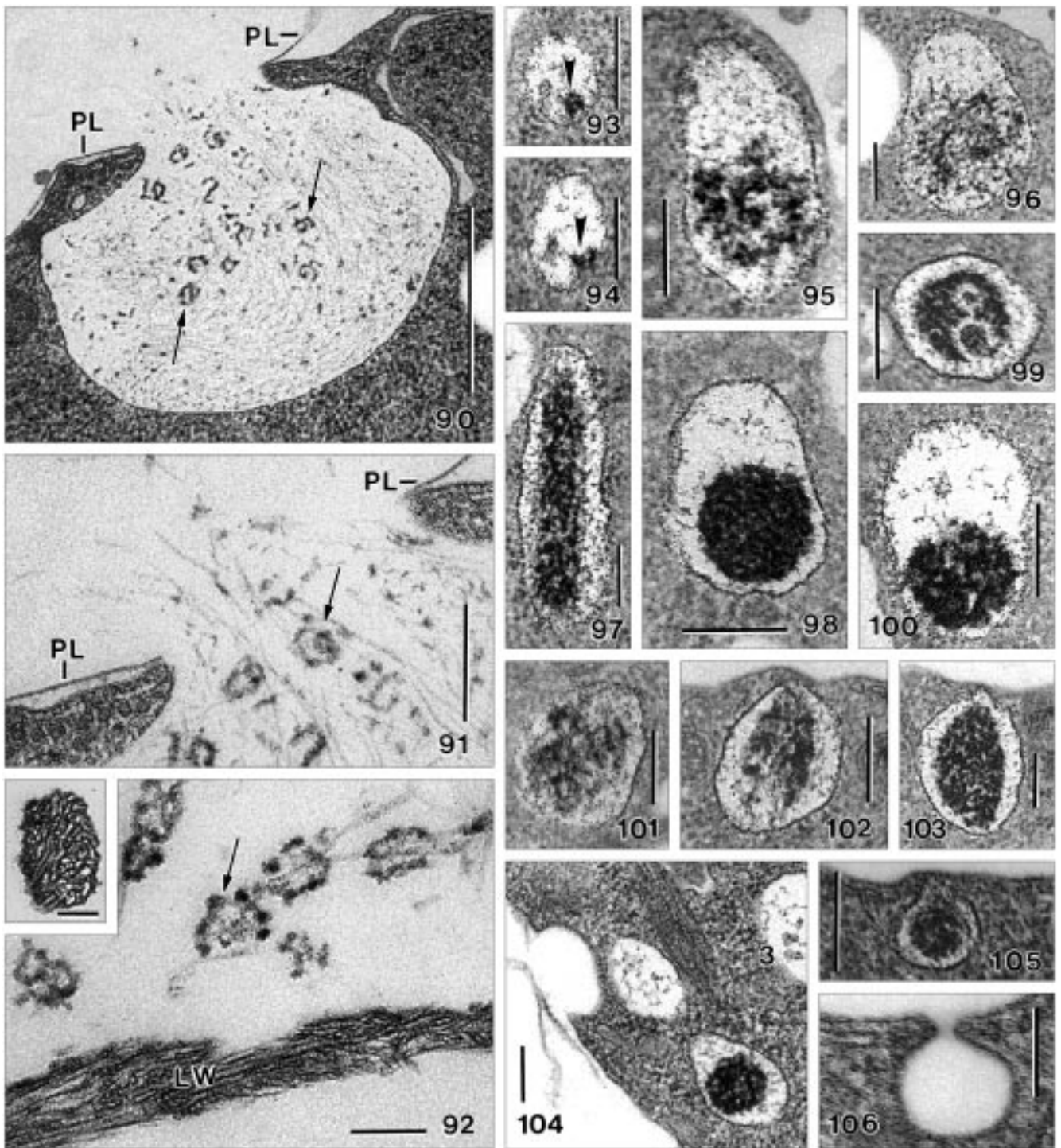
Stage (4): the precursor becomes pyriform again and has an average size of 532×351 nm; the surrounding membrane is more or less wrinkled (Figs 98-100, Table 2). The darkly stained central material described in the previous stages condensed to a narrowly meshed, conspicuous globule with an average size of 269×238 nm. This globule may occupy either the broader or narrower half of the precursor. The rest of the vesicle is filled with wide-meshed fibrogranular material very similar to that found in the previous stages (Figs 98-100).

Stage (5): when the precursor has attached to the cortex of the ciliate, it becomes broadly ellipsoidal showing an average size of 443×293 nm (Figs 101-103, Table 2). As compared to stage (4), the total size slightly decreased from 532×350 nm to 443×293 nm, while the size of the dense core increased from 269×238 to 337×190 nm. This matches the morphological changes, that is, the core loosened and is thus larger and less deeply stained (Figs 101-103).

Stage (6): although being numerous (see above), few extruding (E) precursors were found, indicating that most are released during a very short period. Further, the contents become stainless as soon as the vesicle opens. Thus, we could not follow the further way of the (E) precursor.

Cortex reorganization and perilemma endocytosis

The following data are based on four stage (e) cysts: two of them have a strongly alveolate, wrinkled cortex and few endocytotic vesicles, while the two others have a thin, reduced cortex with many endocytotic vesicles. All cells have small areas where either the original cortex is still present or has been fully reorganized (Fig. 76). Morphometric data of the process and structures described below are shown in Table 3. Briefly, the measurements show that all membranes have a usual thickness (6-7 nm) and four size-classes of vesicles can be distinguished.



Figs 90-106. *Meseres corlissi*, transmission electron micrographs of the extrusion of the (D) precursor (90-92), and the genesis (94-103) and extrusion (104-106) of the (E) precursor. **90-92** - emerging (D) precursor, showing the characteristic curls (arrows) produced by the narrowly meshed areas of the basal net (Fig. 89, arrowheads). The inset shows a transverse section of a branch of the peripheral reticulum, whose fine structure highly resembles that of the lepidosome wall; **93, 94** - stage (1) vesicles of the (E) precursor have a size of 261×202 nm and a unique accumulation of strongly osmiophilic material attached to the membrane (arrowheads); **95, 96** - stage (2) vesicles have a size of 585×382 nm and are pyriform. The wider part is filled with fibrogranular material; **97** - in stage (3), the precursor reaches a size of 533×210 nm. The central portion is filled with strongly osmiophilic material; **98-100** - when approaching stage (4), the precursor becomes pyriform again and has a size of 532×351 nm. The osmiophilic material condensed to a conspicuous globule; **101-103** - in stage (5), the precursor attaches to the cortex and has an average size of 443×293 nm. The core material loosens and thus appears less deeply stained than in stage (4); **104-106** - when extruded, the contents of the (E) precursor become stainless. LW - lepidosome wall, PL - perilemma. Scale bars: 100 nm (92, 106); 200 nm (91, 93-105); 600 nm (90).

During encystment stage (e), that is, when the cell significantly reduces its volume (Foissner *et al.* 2006 and Fig.1) and produces the (E) cyst wall precursor (Figs 93-103), the cortical alveoli double and treble their size and the cortex becomes heavily wrinkled; rarely occur endocytotic vesicles, as described below (Fig. 77). The cortical microtubule sheet has been decomposed earlier, that is, when the cell rounded up. These processes leave back a distinctly altered cortex with a cell membrane and few, very small alveoli (Figs 78, 79, 83). Then, an extraordinary process commences, viz., the formation of innumerable cortical vesicles which endocytose the surplus perilemma produced by the diminution of the cell and the reduction of the ciliary organelles. In the two appropriate cells studied, there were about 100-200 endocytotic events each in a single section through the mid of the cell, plus about 200 just internalized vesicles with decomposing perilemma.

Endocytotic vesicle formation commences with a flat concavity which soon grows and deepens to a bowl-shaped structure with a median size of 228×200 nm (Figs 72, 78-81; Table 3). Frequently, the vesicles are close together, forming breast-like figures (Figs 73, 81). The perilemma does not deepen during vesicle formation and thus covers the vesicle like the lid the pot (Figs 80, 81). Most of the vesicles have the cytoplasmic surface covered by a more or less distinct, electron-dense coat

with an average thickness of 10 nm (Figs 74, 78-81; Table 3). When the vesicles are fully developed, the internalization of the perilemma commences with a minute concavity over the centre of the vesicle (Fig. 80). This concavity grows (Fig. 81), eventually becoming a drop-shaped structure extending into the centre of the vesicle which commences to close by inclining the anterior margin (Figs 72, 74, 75, 82). Concomitantly, the surface coat disappears and then the vesicle pinches off, remaining underneath the cell surface and slightly increasing in size to an average of 352×269 nm (Fig. 72, 74, 81-83; Table 3).

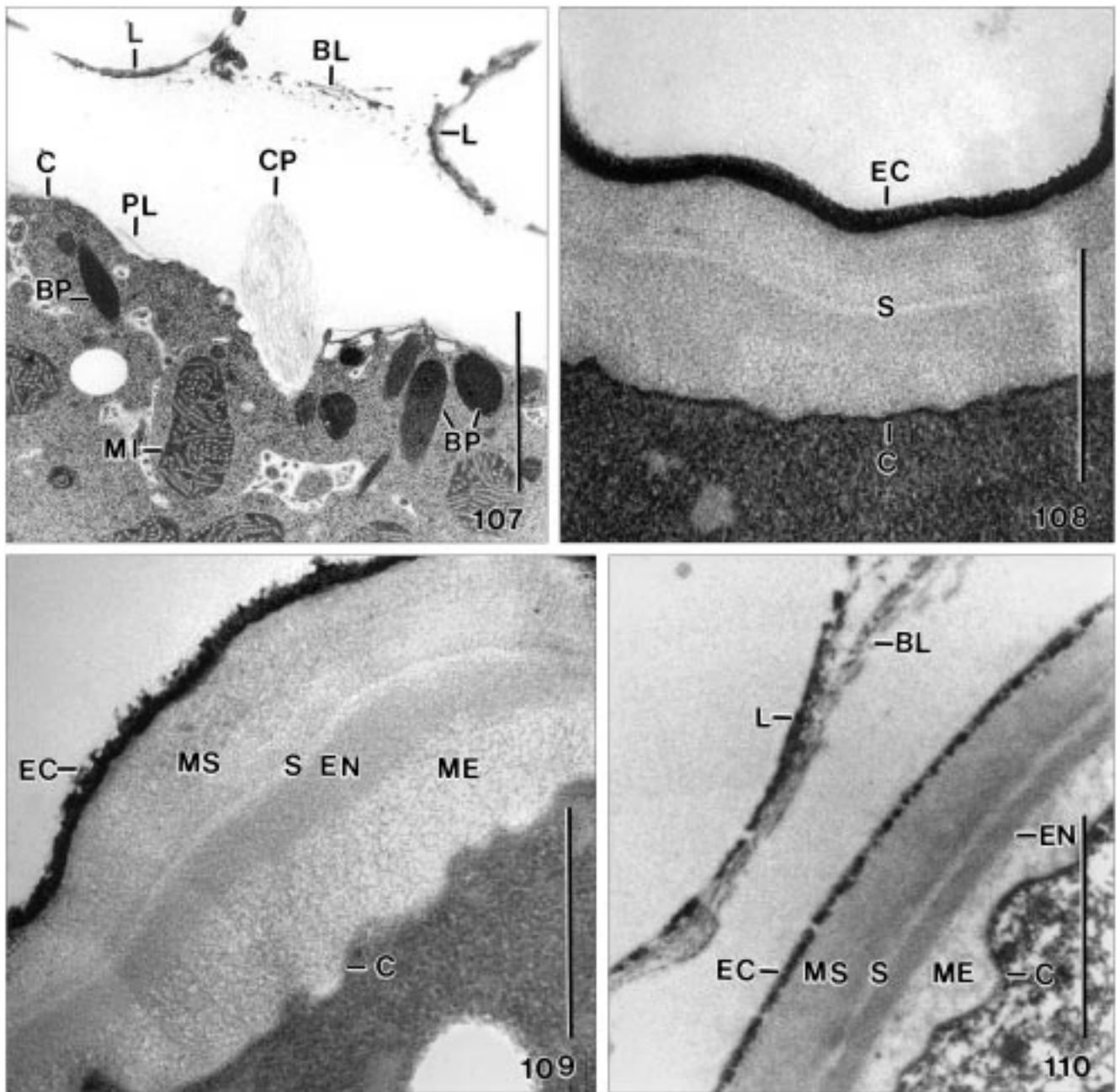
The following stages of perilemma decomposition were reconstructed from hundreds of micrographs. The analysis suggests that the vesicles and their contents become compacted to an average size of 218×157 nm. Thus, they appear dark, often showing myelin figures (Fig. 75). Still the vesicles are in the peripheral $1 \mu\text{m}$ of the cell, where they commence to fuse with each other and to move centripetally, forming bright vacuoles with membrane remnants and an average size of 612×439 nm (Fig. 76, Table 3). These vacuoles then fuse with autophagous vacuoles (Fig. 76).

Formation of basal layer and cyst wall

When the lepidosomes have been released, the encysting cell begins to rotate slowly for some minutes. During this period, an up to $10 \mu\text{m}$ wide, clear, structure-

Table 3. *Meseres corlissi*, morphometric data on reorganization of cortex and perilemma endocytosis. Arabic and Roman numerals ahead of the characteristics correspond to those shown in figure 112. Measurements in nm and from two cysts in encystment stage (e). CV - coefficient of variation in %, M - median, Max - maximum, Min - minimum, n - number of specimens measured, SD - standard deviation, \bar{X} - arithmetic mean.

Characteristics	\bar{X}	M	SD	CV	Min	Max	n
Membrane thickness							
1 Cortex	32.1	33.0	4.6	14.3	24	40	11
2 Perilemma	6.2	7.0	1.0	15.8	5	7	11
3 Forming endocytotic vesicles (without coat)	6.4	6.0	0.9	14.4	5	8	11
4 Membrane plus coat of forming endocytotic vesicles	16.4	16.5	3.5	21.4	12	22	12
5 Internalized vesicles close to cell surface	6.6	6.5	1.3	19.9	5	9	16
6 Perilemma within internalized vesicles	6.8	7.0	1.2	18.2	5	8	13
Size of endocytotic vesicles							
I Fully developed vesicles, length	309.8	288	112	36.2	150	622	30
Fully developed vesicles, depth	209.4	200	80	38.0	100	400	30
II Internalized vesicles close to cortex, length	352.2	333	82	23.3	200	542	30
Internalized vesicles close to cortex, width	269.4	253	73	27.1	156	500	30
III Dark endocytotic vesicles, length	217.7	206	66	30.1	100	356	30
Dark endocytotic vesicles, width	155.6	148	49	31.2	58	250	30
IV Internalized vesicles in cytoplasm, length	612.2	573	162	26.4	367	1083	30
Internalized vesicles in cytoplasm, width	438.5	433	141	32.2	222	900	30



Figs 107-110. *Meseres corlissi*, formation of cyst wall. **107** - extrusion of a (C) precursor (CP; for higher magnifications, see figures 58, 59) in a specimen which has released the lepidosomes (L) and many (B), (C), and (D) precursors. All these materials, except of the lepidosomes and the basal layer, are in the space between basal layer (BL) and ciliate cortex (C), but cannot be seen because they do not stain with the methods used. Thus, the early stages of cyst wall formation could not be followed; **108** - middle stage of cyst wall formation, showing the deeply stained, structureless ectocyst and a thick, fibrogranular layer divided by a narrow, electron-lucent zone (S). The cytoplasm is very dense and poorly preserved in this stage; **109, 110** - a young (109) and a mature (110) cyst wall. They differ mainly by the ectocyst, which is structureless in the former and coarsely granular in the latter. BL - basal layer of pericyst, BP - cyst wall precursor (B), C - cortex of the ciliate, CP - cyst wall precursor (C), EC - ectocyst, EN - endocyst, L - lepidosomes, ME - metacyst, MI - mitochondrium, MS - mesocyst, PL - perilemma of the ciliate cortex, S - space. Scale bars: 600 nm (108, 109); 2000 nm (107, 110).

less zone, recognizable mainly due to adhering bacteria, develops around the globular cell (Foissner *et al.* 2006). This zone is formed by the materials released from cyst wall precursors (B-E).

Although we sectioned five appropriate specimens, we could not observe the formation of the cyst wall in the electron microscope, partially because the materials released by the wall precursors became stainless, as reported above. The wall either had not yet assembled or assemblage was almost finished, that is, we did not find transitions between the stages shown in Figures 107 and 108. Thus, cyst wall formation must be a fast “condensation” process, including a far-reaching restructuring of the materials so that they become visible again in the electron microscope. In this process, the slow rotation of the cell possibly mixes and transports the materials to the specific positions (Fig. 1, Foissner *et al.* 2006). What we could observe, is described in the following paragraphs.

The basal layer, upon which the lepidosomes lie or are partially embedded, is the proximal, denser portion of the slimy coat surrounding the cyst of *M. corlissi* (Foissner 2005; Foissner *et al.* 2005, 2006; Figs 27, 28, 107, 110). The developing lepidosomes are enclosed by a membrane which is very near to the lepidosome wall; thus, no space remains for slime (Foissner *et al.* 2006). Likewise, the lepidosome cavity does not contain slime because it does not stain with alcian blue (Foissner *et al.* 2005). Thus, the mucous coat of the *Meseres* cyst must be produced by one or several cyst wall precursors. Figures 27-31 and 90-92 indicate that the basal layer, and thus likely the entire slime coat, is formed by the (B) and (D) precursors because remnants (membranous sheets, curls) of them are recognizable in that layer. However, we cannot exclude that parts of the (B) and (D) precursors contribute to other layers of the cyst wall, too.

The just assembled (young) cyst wall is considerably thinner (\bar{x} 737 nm, Min 617 nm, Max 790 nm, n 5) than the mature wall (\bar{x} 1241 nm, Foissner 2005), but already shows the bright zone between mesocyst and endocyst (Figs 108, 110). Basically, two layers are recognizable in this stage (Fig. 108): the deeply stained, thin, structureless ectocyst (coarsely granular in the mature cyst; Fig. 110 and Foissner 2005) and a lightly stained, thick, fibrogranular layer divided by a narrow, electron-lucent zone present also in the mature wall (Fig. 110). In a later stage (Fig. 109), which is already very similar to the mature wall (Fig. 110), all cyst layers are recognizable,

but the ectocyst is still structureless (coarsely granular in the mature cyst; Fig. 110); the mesocyst is fibrogranular (usually with herring-bone pattern in the mature cyst); and the metacyst is finely reticular (coarsely reticular and often granular in the mature cyst; Fig. 110).

DISCUSSION

Genesis of the cyst wall precursors (Fig. 111)

According to Gutiérrez *et al.* (2003), “There is no reliable information on the origin of resting cyst wall precursors in the ciliate cytoplasm, although cytochemical evidence supports the notion that the origin of the cyst wall precursors is from ER and/or Golgi complex (Calvo *et al.* 1986)”. However, Walker *et al.* (1989) provided convincing electron micrographs that the cyst wall precursor of a peritrich ciliate, *Telotrochidium henneyi*, develops pairwise in dilated Golgi cisterns. This has been confirmed in *M. corlissi*, where the (A) wall precursor (= lepidosomes) originates the same way (Foissner *et al.* 2006). The present data show that cyst wall precursor (C) of *M. corlissi* also originates in Golgi vesicles (Figs 32-36). However, there is a slight difference: cyst wall precursor (A) originates pairwise in the dilated ends of Golgi cisterns, while cyst wall precursor (C) forms by growth of individual Golgi vesicles. Unfortunately, we could not find out the origin of cyst wall precursors (B), (D) and (E). Likely, they are also produced from saccules and vesicles of the Golgi complex, just like scales and various other surface structures of protists (Bovee 1991, Vickermann *et al.* 1991).

We could not clarify precursor growth; it is not vesicular endocytosis, suggesting material uptake across the precursor membrane *via* an active, carrier-mediated process.

Number and morphology of cyst wall precursors in ciliates (Fig. 111)

Literature data have been reviewed by Gutiérrez and Martín-González (2002) and Gutiérrez *et al.* (2003). Briefly, the cyst wall of ciliates consists of 2-4 layers (3-5 if the pericyst is recognized as a distinct layer; Foissner 2005), depending on the group of ciliates; rarely, there are differences between the species of a genus or the genera of a family. These layers are the pericyst, ectocyst, mesocyst, endocyst and metacyst. Usually,

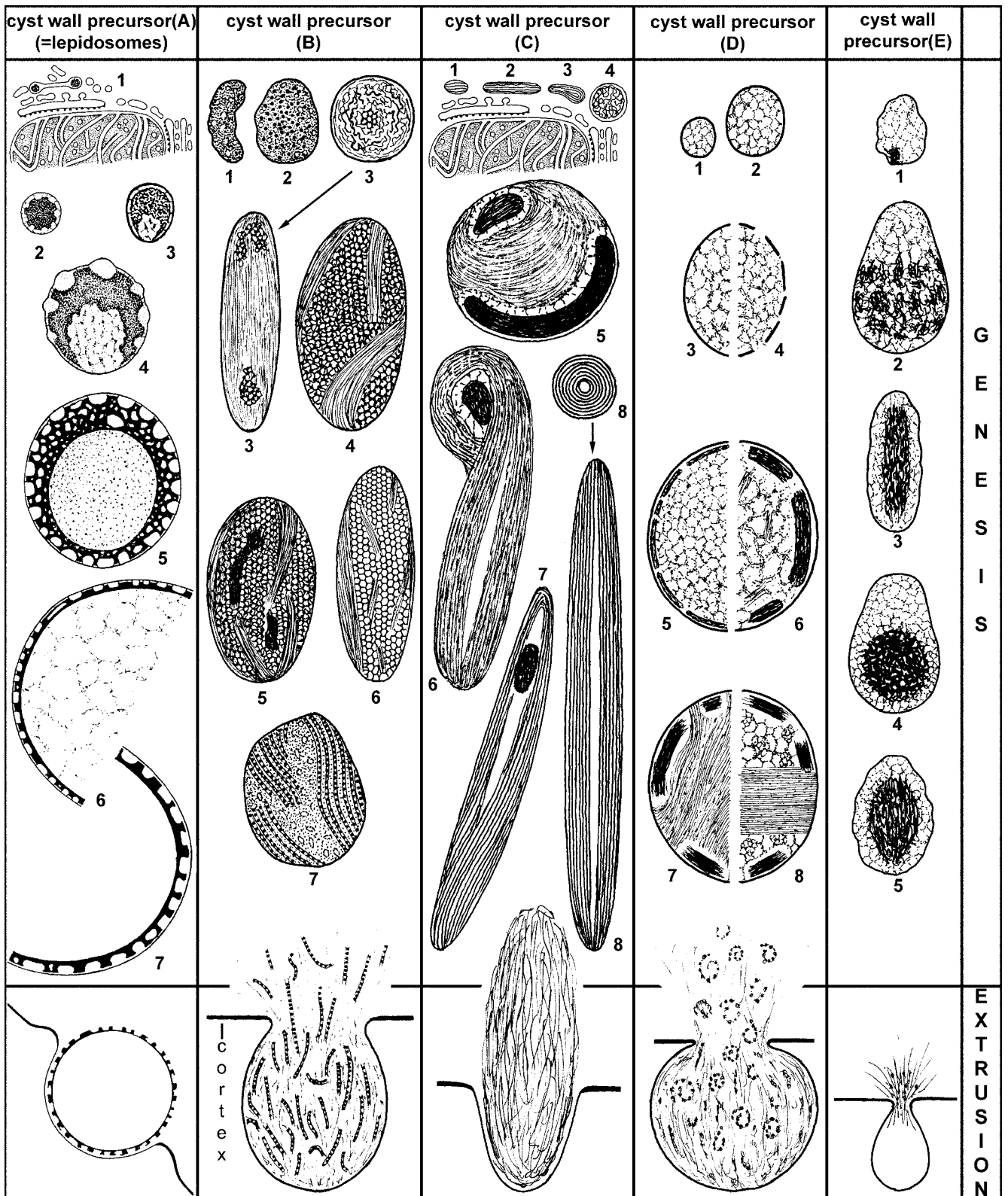


Fig. 111. *Meseres corlissi*, scheme of genesis and extrusion of cyst wall precursors (A-E). Genesis of precursor (A) is described in Foissner *et al.* (2006). Figures roughly drawn to scale within individual files. Numerals denote developmental stages as described in the text.

each layer originates from a distinct precursor whose development, unfortunately, rarely has been documented in detail.

With few exceptions, the cyst wall precursors are either mucocysts, for instance, in *Tetrahymena rostrata* (McArdle *et al.* 1980) and *Colpoda magna* (Frenkel 1994), or small ($\leq 1\mu\text{m}$) vesicles with fibrogranular or amorphous contents, for instance, in *Gonostomum* (Walker and Hoffman 1985) and *Telotrochidium henneguyi* (Walker *et al.* 1989). Well known exceptions are the plate-like ectocyst precursors of several stichotrichine spirotrichs (e.g. *Oxytricha*, *Coniculostomum*) and the hairpin-shaped clathrocysts which produce the mesocyst of *Didinium nasutum* (Holt and Chapman 1971). These precursors are some μm in size and show distinct developmental stages, just as those of *Meseres*.

Meseres corlissi highly resembles stichotrichine spirotrichs in the number of cyst wall precursors and wall layers. In contrast, the morphology of the wall precursors is entirely different from those described as yet, both in the developing and mature state (Fig. 111). There are some superficial similarities, for instance, the membranous structure of the (C) precursor resembles the ectocyst precursor of the stichotrichs. However, their genesis is different and when extruded the (C) precursor of *Meseres* dissolves and becomes stainless, while the plates of the stichotrichine ectocyst precursor remain structurally intact and form the lamellar ectocyst (Gutiérrez *et al.* 1983, 2003). The (E) precursor resembles the cyst wall precursor vesicles of several ciliates, for instance, *Gonostomum* (Walker and Hoffman 1985) and *Colpoda magna* (Frenkel 1994), but the details of genesis and fine structure are different. Accordingly, we conclude that the oligotrichine spirotrichs are a very distinct group of ciliates differing from other ones not only by their general morphology, but also in the genesis and mature structure of the cyst wall precursors.

Release of cyst wall precursors (Fig. 111)

Detailed data on the release of the cyst wall precursors are lacking in ciliates, except for *M. corlissi*, where Foissner *et al.* (2006) showed that cyst wall precursor (A), i.e., the lepidosomes are released by classical exocytosis (Plattner and Hentschel 2002, Becker *et al.* 2006), that is, the surrounding membrane fuses with the cortex membranes and is integrated into the newly forming cortex. Here, we show the same for the (B) precursor (Figs 27, 29), the (C) precursor (Fig. 59) and the (D) precursor (Fig. 90), while data for the (E)

precursor are insufficient due to problems in differentiating the release stages from perilemma endocytosis. Accordingly, exocytosis of the cyst wall precursors is different from extrusome exocytosis, where the enveloping membrane is recycled in the cytoplasm (Hausmann 1978, Vickerman *et al.* 1991, Peck *et al.* 1993, Plattner and Kissmehl 2003). In *Meseres*, augmentation of the surface area by the precursor membranes makes sense because about 1000 cyst wall precursors with a diameter of up to 15 μm (lepidosomes) are released almost concomitantly. The exocytotic openings produced occupy an average of about 87 % of the surface of the forming cyst (calculated surface area of *Meseres* without peristomial bottom where few or no precursors are released: $\sim 8000\mu\text{m}^2$; 200 lepidosomes with an average diameter of 6 μm : $\sim 5700\mu\text{m}^2$; 800 (B, C, D) precursors with an average diameter of 1 μm : $\sim 1260\mu\text{m}^2$). Thus, resealing of the exocytotic openings requires a lot of membrane obviously provided by the vesicles containing the cyst wall precursors. Certainly, further investigations have to clear the details of the process, but our basal observation that the membrane of the precursors is integrated into the newly forming cortex is well documented (Figs 27, 29, 59, 90, 111 and Figs 52-57 in Foissner *et al.* 2006).

We could not clarify the precursor transport and release *s. str.* The cyst wall precursors of the stichotrichine ciliate *Gastrostyla steinii* and the scales of chrysophytes are guided to the cortex by microtubules (Walker *et al.* 1980, Vickerman *et al.* 1991). In *M. corlissi*, microtubules or other fibres are not recognizable. However, there is fast rotation of the cell just before the precursors are released, suggesting that they are transported by centrifugal forces to the cell periphery. The release *s. str.* of the lepidosomes and the contents of the vesicles may be achieved by the cell turgor, which probably increases before extrusion, because the cell becomes slightly inflated, just like it would take a deep breath (Foissner *et al.* 2006).

Formation of cyst wall

One of the firm findings in ciliate cyst research is the sequential formation of the cyst wall precursors and their successive secretion to generate the individual cyst layers (Grimes 1973; Gutiérrez *et al.* 1983, 2003; Calvo *et al.* 1986). *Meseres corlissi* breaks this rule: four of the five wall precursors are generated and released almost concomitantly, and the cyst wall suddenly “condenses” out off the stainless mass formed by the extruded contents of the wall precursors.

Unfortunately, authors often do not comment on cyst wall assemblage *s. str.* However, those studies which do show that the secreted precursors basically maintain their structure and visibility, that is, stain with the ordinary methods. Good examples are *Didinium nasutum* (Holt and Chapman 1971), *Colpoda magna* (Frenkel 1994), *Oxytricha fallax* (Grimes 1973), *Laurentiella acuminata* (Gutiérrez *et al.* 1983), and *Coniculostomum monilata* (Kamra and Sapra 1993). This contrasts *M. corlissi*, where the released precursors change their structure so distinctly that they become invisible (Figs 27, 59, 90, 105, 107), except of precursor(A) which, however, is assembled within the cell (Foissner *et al.* 2006).

We could not observe which precursors form the individual cyst layers of *M. corlissi* because the materials become stainless when released. Possibly, this is unique to *Meseres* or the oligotrichs. However, it might occur also in some other ciliates, for instance, in *Oxytricha bifaria*, where the seemingly empty pericellular space could contain stainless mesocyst material because all other cyst layers have already formed (Verni *et al.* 1984; Figs 5, 6, 9).

Three further general aspects on cyst wall precursors and wall assemblage can be extracted from our investigations and the literature. First, the cyst wall can be formed (i) from precursors generated *de novo*, for instance, in *Meseres* and many other ciliates (Gutiérrez *et al.* 2003); (ii) mainly by organelles present in the morphostatic cell, for instance, the mucocysts in *Tetrahymena rostrata* (McArdle *et al.* 1980); (iii) by a combination of precursors and organelles present in the morphostatic cell, for instance, in *Colpoda magna* (Frenkel 1994) and *Engelmanniella mobilis* (Wirnsberger-Aeschl *et al.* 1990); and (iv) without recognizable, membrane-bound precursors, for instance, in the parasitic ciliate *Hyalophysa chattoni* (Landers 1991). Second, the cyst wall is assembled either outside the cell's cortex (usual way, Gutiérrez *et al.* 2003) or part of the wall is assembled within the cell, for instance, the lepidosomes of *Meseres* (Foissner *et al.* 2006) and *Halteria* (Foissner, unpubl.). Third, the cyst wall forms outside the cell (usual way, as in *Meseres*) or subcortically (known only from *Colpoda steinii*, Ruthmann and Kuck 1985). There are some reports that the cyst wall forms between the cell membrane and the perilemma in stichotrichine spirotrichs (Grimes 1973, Matsusaka 1976, Walker *et al.* 1980, Calvo *et al.* 1986). However, convincing micrographs are lacking (Foissner *et al.* 2006 and next chapter).

Cortex reorganization and perilemma endocytosis (Fig. 112)

To our best knowledge, cortex reorganization and/or perilemma endocytosis have not been reported in encysting ciliates. This is surprising, considering that body volume (size) and body surface are usually considerably reduced. For instance, the cyst volume of *M. corlissi* is only 28% of that of the vegetative cell and only 5% in *Opisthonecta*, a peritrich ciliate (Foissner *et al.* 2006). Even more surprising is the absence of reports on perilemma endocytosis in several well investigated stichotrichs, for instance, *Oxytricha* (Grimes 1973), *Laurentiella* (Gutiérrez *et al.* 1983) and *Coniculostomum* (Kamra and Sapra 1993). This indicates that perilemma endocytosis is a specific trait of oligotrichs. However, endocytosis occurs only during a short period of the encystment process (Fig. 1). Thus, it cannot be excluded that previous studies missed it by bad luck.

Preservation of the fine structure is difficult in resting cysts, even if the protecting wall has not yet formed, because encystment involves a complete restructuring of the cell which thus becomes fragile and difficult to fix. None the less, we are sure that our micrographs (Figs 76-79) show cortex reorganization because the wrinkled cortex and the large alveoli appear just when the cell significantly reduces its size and thus much surplus cortex has to be removed. The reorganization occurs without special anlagen and is thus unspectacular and rather difficult to recognize, possibly explaining the lack of previous reports.

The perilemma is a unit membrane-like structure covering body and cilia of oligotrichine and stichotrichine spirotrichs, except of the curious lack in *Halteria*, the closest relative of *Meseres* (Fauré-Fremiet and Ganier 1970, Grain 1972, Laval-Peuto 1975, Bardele 1981, Wirnsberger-Aeschl *et al.* 1989, Katz *et al.* 2005). In *M. corlissi*, up to five perilemma membranes occur in the vegetative specimens and two in cystic cells (Foissner 2005). Our investigations show that only part of the perilemma is removed by endocytosis, likely mainly the surplus portion originating from body size and cilia reduction.

In conventional electron micrographs, there is no absolute marker for distinguishing endocytosis and exocytosis. However, often this is possible when other aspects are taken into account. In *Meseres*, we interpret the cortical vesicles as an endocytotic process for the following reasons: (i) Cortex reorganization and perilemma

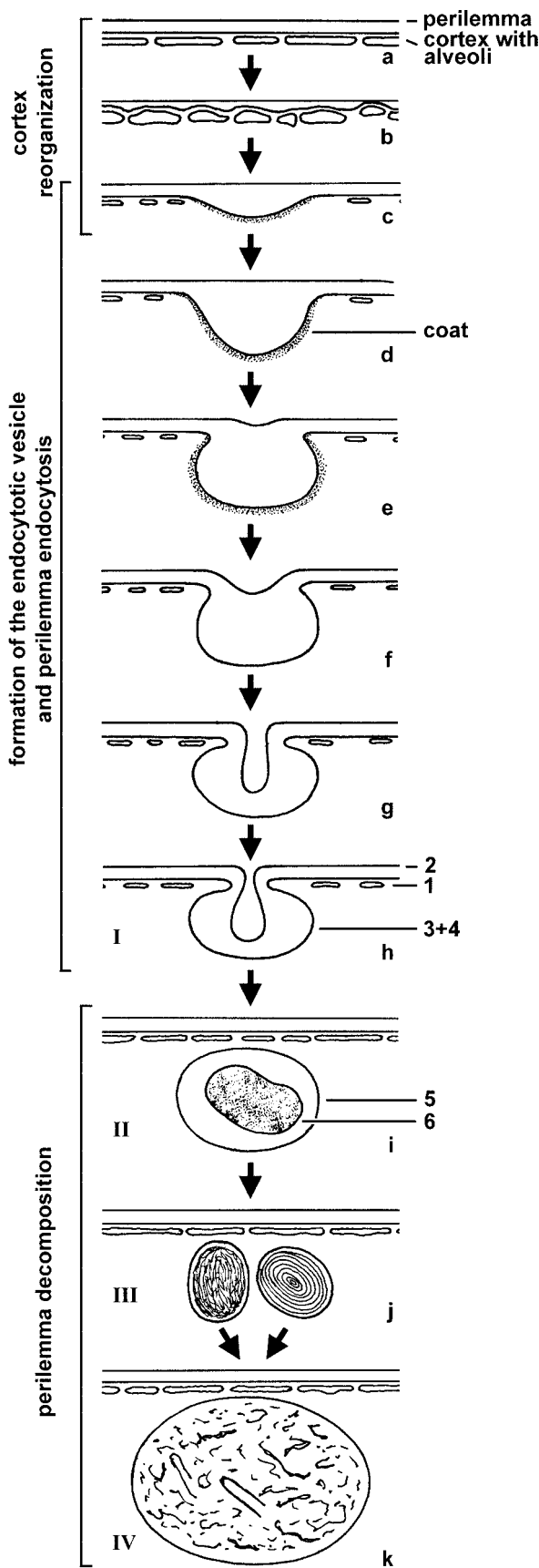


Fig. 112. *Meseres corlissi*, scheme of reorganization of cortex (a-c), formation of the endocytotic vesicle and perilemma endocytosis (c-h), and perilemma decomposition (i-k). Drawn to scale, according to data compiled in Table 3. Unit membranes shown as simple lines. Arabic (1-6) and Roman (I-IV) numerals correspond to structures measured in Table 3. See text and discussion for more detailed explanations.

endocytosis take place during encystment stage (e), that is, when the cell significantly reduces its size (Foissner *et al.* 2006), decomposes the ciliary organelles, and the number of autophagous vacuoles reaches a maximum (Fig. 1); (ii) The vesicles are coated only during formation and only on the cytoplasmic surface (Figs 74, 78, 79); (iii) The vesicles are most numerous in the oral area, where plenty of ciliary perilemma must be removed; (iv) The vesicles contain membrane pieces. To our best knowledge, it never has been described that membrane pieces are produced deep in the cytoplasm, transported to the cell's surface, and then integrated into an existing membrane; (v) The vesicles develop to vacuoles with myelin figures, which are typical for decomposing membranes; (vi) Last but not least, the micrographs (Figs 72-83) strongly suggest endocytosis, that is, progress of the processes as shown in the scheme (Fig. 112). This applies especially for the stages shown in figures 80 and 81, which can occur only during an endocytotic process.

No data are available on the composition and function of the perilemma as well as how it is derived and replenished. Lynn and Corliss (1991) speculate that it may be a special kind of fixation artifact of the glycocalyx, while Bardele (1981) proposes: "I believe that the perilemma is a temporary structure which is renewed quite often, for numerous layers of the perilemma are usually seen in the buccal cavity. It is not known whether the perilemma is involved in food gathering under certain physiological conditions, for example, starvation, or is a prerequisite to encystation, where it certainly forms the outer layer during early stages of cyst formation (Grimes 1973)". As concerns participation in cyst wall formation, the evidences are weak, that is, convincing electron micrographs are lacking that the ectocyst precursor is entrapped between the perilemma and the cell membrane. And it contradicts the observations on *Meseres*, where the perilemma disappears at the sites where the wall precursors leave the cell (Figs 59, 90, 91, 107 and Foissner *et al.* 2006). Our investigations also rule out that the perilemma is a temporary structure or a fixation artifact because it is present throughout the life cycle and becomes reduced by endocytosis with defined decomposition stages in the internalized vesicles (Fig. 75).

Some function in food gathering cannot be excluded, but is unlikely considering that it covers the whole body. Thus, nothing remains except of the morphological facts. Our investigations suggest that structure and composition of the perilemma are considerably different from those of ordinary cortex membranes; otherwise, it would not need so prominent endocytosis to be removed.

Phylogenetic implications

The compilation above shows a considerable diversity of the processes associated with cyst wall formation in ciliated protozoa. Likely, many more possibilities remain to be discovered. If this diversity is added to that of overall cyst morphology (e.g., wall ornamentation), cyst wall composition (e.g., with or without chitin) and cell restructuring (e.g., the infraciliature may be maintained or partially or completely resorbed), an overwhelming diversity emerges which should contain considerable ecological and phylogenetic information; unfortunately, the message is only partially understood, likely because detailed data on resting cyst formation and structure are available from less than 40 species (Gutiérrez *et al.* 2003). For instance, when one compares the very different modes of cyst wall formation in *Colpoda steinii* (Ruthmann and Kuck 1985) and *C. magna* (Frenkel 1994), then it seems likely that both belong to different genera or even families, although taxonomists consider them as congeneric (Foissner 1993).

When discussing the classification of the halteriine spirotrichs, to which *Meseres* belongs (Katz *et al.* 2005), Foissner *et al.* (2004) reached the conclusion that further data are necessary to decide whether they are oligotrichine or stichotrichine spirotrichs, as suggested by the ontogenetic, respectively, molecular investigations. The present study supports the classical view that the halteriids belong to the oligotrichs because the cyst wall precursors are quite different from those of the stichotrichs. Specifically, *Meseres* lacks the highly characteristic stacks of membrane-like ectocyst precursors of the stichotrichine spirotrichs, and thus has a different mature ectocyst (Foissner 2005). Likewise, there are no similarities to the urostylid ectocyst (Rios *et al.* 1985), while the kahliellid ectocyst is as thin as that of *Meseres* and thus looks rather similar (Foissner and Foissner 1987). However, it is composed of a membranous sheet in *Kahliella*, while coarsely granular in *Meseres* (Foissner 2005).

Acknowledgements. Financial support was provided by the Austrian Science Foundation, FWF project P 16796-B06. The technical

assistance of Andreas Zankl and Mag. Birgit Peukert is greatly acknowledged.

REFERENCES

- Bardele C. F. (1981) Functional and phylogenetic aspects of the ciliary membrane: a comparative freeze-fracture study. *BioSystems* **14**: 403-421
- Becker, W. M., Kleinsmith L. J., Hardin J. (2006) *The World of the Cell*, 6th ed. Pearson, San Francisco and Toronto
- Berger H. (1999) Monograph of the Oxytrichidae (Ciliophora, Hypotrichia). Kluwer, Dordrecht, Boston, London
- Bovee E. C. (1991) Sarcodina. *Microsc. Anat. Invert.* **1**: 161-259
- Calvo P., Torres A., Perez-Silva J. (1986) Ultrastructural and cytochemical study of the encystment in the hypotrichous ciliate *Histiculus similis*. *Arch. Protistenk.* **132**: 201-211
- Chessa M. G., Delmonte Corrado M. U., Carcupino M., Pelli P. (1994) Ultrastructural cortical aspects of cell differentiation during long-term resting encystment in *Colpoda inflata*. In: Contribution to Animal Biology (Eds. R. Argano, C. Cirotto, E. Grassi Milano, L. Masfrolia). Halocynthia Association, Palermo, 169-172
- Corliss J. O. (1979) *The Ciliated Protozoa. Characterization, Classification and Guide to the Literature*. 2 ed. Pergamon Press, Oxford, New York, Toronto, Sydney, Paris, Frankfurt
- Corliss J. O., Esser S. C. (1974) Comments on the role of the cyst in the life cycle and survival of free-living protozoa. *Trans. Am. microsc. Soc.* **93**: 578-593
- Fauré-Fremiet E. (1948) Le rythme de marée du *Strombidium oculatum* Gruber. *Bull. biol. France Belg.* **82**: 3-23
- Fauré-Fremiet E., Ganier M.-C. (1970) Structure fine du *Strombidium sulcatum* Cl. et L. (Ciliata Oligotrichida). *Protistologica* **6**: 207-223
- Foissner W. (1984) Infraciliatur, Silberliniensystem und Biometrie einiger neuer und wenig bekannter terrestrischer, limnischer und mariner Ciliaten (Protozoa: Ciliophora) aus den Klassen Kinetofragminophora, Colpodea und Polyhymenophora. *Stapfia, Linz* **12**: 1-165
- Foissner W. (1993) Colpodea (Ciliophora). *Protozoenfauna* **4**: I-X + 798 p
- Foissner W. (2005) The unusual, lepidosome-coated resting cyst of *Meseres corlissi* (Ciliophora: Oligotricha): transmission electron microscopy and phylogeny. *Acta Protozool.* **44**: 217-230
- Foissner I., Foissner W. (1987) The fine structure of the resting cysts of *Kahliella simplex* (Ciliata, Hypotrichida). *Zool. Anz.* **218**: 65-74
- Foissner W., Agatha S., Berger H. (2002) Soil ciliates (Protozoa, Ciliophora) from Namibia (Southwest Africa), with emphasis on two contrasting environments, the Etosha Region and the Namib Desert. *Denisia* **5**: 1-1459
- Foissner W., Moon-van der Staay S.Y., van der Staay G. W. M., Hackstein J. H. P., Krautgartner W.-D., Berger H. (2004) Reconciling classical and molecular phylogenies in the stichotrichines (Ciliophora, Spirotrichea), including new sequences from some rare species. *Europ. J. Protistol.* **40**: 265-281
- Foissner W., Müller H., Weisse T. (2005) The unusual, lepidosome-coated resting cyst of *Meseres corlissi* (Ciliophora: Oligotricha): light and scanning electron microscopy, cytochemistry. *Acta Protozool.* **44**: 201-215
- Foissner W., Pichler M., AL-Rasheid K., Weisse T. (2006) The unusual, lepidosome-coated resting cyst of *Meseres corlissi* (Ciliophora: Oligotricha): encystment and genesis and release of the lepidosomes. *Acta Protozool.* **45**: 323-338
- Frenkel M. A. (1994) The cyst wall formation in *Tillina magna* (Ciliophora, Colpodidae). *Arch. Protistenk.* **144**: 17-29
- Grain J. (1972) Etude ultrastructurale d'*Halteria grandinella* O.F.M., (Cilié Oligotriche) et considérations phylogénétiques. *Protistologica* **8**: 179-197
- Grimes G. W. (1973) Differentiation during encystment and excystment in *Oxytricha fallax*. *J. Protozool.* **20**: 92-104

- Gutiérrez J. C., Martín-González A. (2002) Ciliate encystment-encystment cycle: a response to environmental stress. In: *Microbial Development Under Environmental Stress* (Ed. J. C. Gutiérrez). Research Signpost 37/661(2), Trivandrum - 695 023, Kerala, India, 29-49
- Gutiérrez J. C., Torres A., Perez-Silva J. (1983) Structure of cyst wall precursors and kinetics of their appearance during the encystment of *Laurentiella acuminata* (Hypotrichida, Oxytrichidae). *J. Protozool.* **30**: 226-233
- Gutiérrez J. C., Diaz S., Ortega R., Martín-González A. (2003) Ciliate resting cyst walls: a comparative review. *Recent Res. Devel. Microbiol.* **7**: 361-379
- Hausmann K. (1978) Extrusive organelles in protists. *Int. Rev. Cyt.* **52**: 197-276
- Holt P. A., Chapman G. B. (1971) The fine structure of the cyst wall of the ciliated protozoon *Didinium nasutum*. *J. Protozool.* **18**: 604-614
- Jonsson P. R. (1994) Tidal rhythm of cyst formation in the rock pool ciliate *Strombidium oculatum* Gruber (Ciliophora, Oligotrichida): a description of the functional biology and an analysis of the tidal synchronization of encystment. *J. Exp. Mar. Biol. Ecol.* **175**: 77-103
- Kamra K., Sapra G. R. (1993) Morphological and ultrastructural changes during encystment in *Coniculostomum monilata* (Ciliophora, Hypotrichida, Oxytrichidae). *Zoology* **3**: 273-302
- Katz L. A., McManus G. B., Snoeyenbos-West O. L. O., Griffin A., Pirog K., Costas B., Foissner W. (2005) Reframing the "Everything is everywhere" debate: evidence for high gene flow and diversity in ciliate morphospecies. *Aquat. Microb. Ecol.* **41**: 55-65
- Kim Y.-O., Taniguchi A. (1995) Excystment of the oligotrich ciliate *Strombidium conicum*. *Aquat. Microb. Ecol.* **9**: 149-156
- Landers S. C. (1991) The fine structure of secretion in *Hyalophysa chattoni*: formation of the attachment peduncle and the chitinous phoretic cyst wall. *J. Protozool.* **38**: 148-157
- Laval-Peuto M. (1975) Cortex, périlemme et réticulum vésiculeux de *Cyrtarocylys brandti* (cilié tintinnide). Les ciliés à périlemme. *Protistologica* **11**: 83-98
- Lynn D. H., Corliss J. O. (1991) Ciliophora. *Microsc. Anat. Invert.* **1**: 333-467
- Matsusaka T. (1976) An ultrastructural study of encystment in the hypotrichous ciliate *Pleurotricha* sp. *Kumamoto J. Sci., Biol.* **13**: 13-26
- McArdle E. W., Bergquist B. L., Ehret C. F. (1980) Structural changes in *Tetrahymena rostratum* during induced encystment. *J. Protozool.* **27**: 388-397
- Montagnes D. J. S., Lowe C. D., Poulton A., Jonsson P. R. (2002) Redescription of *Strombidium oculatum* Gruber 1884 (Ciliophora, Oligotrichia). *J. Eukaryot. Microbiol.* **49**: 329-337
- Müller H. (1996) Encystment of the freshwater ciliate *Pelagostrombidium fallax* (Ciliophora, Oligotrichida) in laboratory culture. *Aquat. Microb. Ecol.* **11**: 289-295
- Müller H. (2002) Laboratory study of the life cycle of a freshwater strombidiid ciliate. *Aquat. Microb. Ecol.* **29**: 189-197
- Müller H., Foissner W., Weisse T. (2006) Role of soil in the life cycle of *Meseres corlissi* (Ciliophora: Oligotrichea): experiments with two clonal strains from the type locality, an astatic meadow pond. *Aquat. Microb. Ecol.* **42**: 199-208
- Peck R. K., Swiderski B., Tourmel A.-M. (1993) Involvement of the trans-Golgi network, coated vesicles, vesicle fusion, and secretory product condensation in the biogenesis of *Pseudomicrothorax* trichocysts. *Adv. Cell Molec. Biol. Memb.* **2**: 1-25
- Petz W., Foissner W. (1992) Morphology and morphogenesis of *Strombidium caudatum* (Fromentel), *Meseres corlissi* n. sp., *Halteria grandinella* (Müller), and *Strombidium rehwaldi* n. sp., and a proposed phylogenetic system for oligotrich ciliates (Protozoa, Ciliophora). *J. Protozool.* **39**: 159-176 ed. Thieme, Stuttgart, New York
- Plattner H., Kissmehl R. (2003) Molecular aspects of membrane trafficking in *Paramecium*. *Int. Rev. Cyt.* **232**: 185-216
- Reid P. C. (1987) Mass encystment of a planktonic oligotrich ciliate. *Mar. Biol.* **95**: 221-230
- Reid P. C., John A. W. G. (1978) Tintinnid cysts. *J. mar. biol. Ass. U.K.* **58**: 551-557
- Reid P. C., John A. W. G. (1983) Resting cysts in the ciliate class Polyhymenophorea: phylogenetic implications. *J. Protozool.* **30**: 710-713
- Rios R. M., Torres A., Calvo P., Fedriani C. (1985) The cyst of *Urostyla grandis* (Hypotrichida, Urostylidae): ultrastructure and evolutionary implications. *Protistologica* **21**: 481-485
- Ruthmann A., Kuck A. (1985) Formation of the cyst wall of the ciliate *Colpoda steinii*. *J. Protozool.* **32**: 677-682
- Sitte P., Ziegler H., Ehrendorfer F., Bresinsky A. (1991) Lehrbuch der Botanik. Fischer, Stuttgart
- Verni F., Rosati G., Ricci N. (1984) The cyst of *Oxytricha bifaria* (Ciliata Hypotrichida). II. The ultrastructure. *Protistologica* **20**: 87-95
- Vickerman K., Brugerolle G., Mignot J.-P. (1991) Mastigophora. *Microsc. Anat. Invert.* **1**: 13-159
- Walker G. K., Hoffman J. T. (1985) An ultrastructural examination of cyst structure in the hypotrich ciliate *Gonostomum* species. *Cytobios* **44**: 153-161
- Walker G. K., Maugel T. K., Goode D. (1980) Encystment and excystment in hypotrich ciliates I. *Gastrostyla steinii*. *Protistologica* **16**: 511-524
- Walker G. K., Edwards C. A., Suchard S. J. (1989) Encystment in the peritrich ciliate *Telotrochidium henneguysi*. *Cytobios* **59**: 7-18
- Weisse T. (2004) *Meseres corlissi*: a rare oligotrich ciliate adapted to warm water and temporary habitats. *Aquat. Microb. Ecol.* **37**: 75-83
- Wirnsberger-Aeschl E., Foissner W., Foissner I. (1989) Morphogenesis and ultrastructure of the soil ciliate *Engelmanniella mobilis* (Ciliophora, Hypotrichida). *Europ. J. Protistol.* **24**: 354-368
- Wirnsberger-Aeschl E., Foissner W., Foissner I. (1990) Natural and cultured variability of *Engelmanniella mobilis* (Ciliophora, Hypotrichida); with notes on the ultrastructure of its resting cyst. *Arch. Protistenk.* **138**: 29-49
- Xu K., Foissner W. (2005) Descriptions of *Protospathidium serpens* (Kahl, 1930) and *P. fraterculum* n. sp. (Ciliophora, Haptorina), two species based on different resting cyst morphology. *J. Eukaryot. Microbiol.* **52**: 298-309

Received on 11th July, 2006; revised version on 29th August, 2006; accepted on 6th October, 2006